ANKARA YILDIRIM BEYAZIT UNIVERSITY

GRADUATE SCHOOL OF NATURAL AND APPLIED SCIENCES

STEERABLE FILTER IN FREQUENCY DOMAIN WITH ROSE CURVE

Ph.D. Thesis by

Ömer MİNTEMUR

Department of Computer Engineering

August, 2021

ANKARA

STEERABLE FILTER IN

FREQUENCY DOMAIN WITH ROSE CURVE

A Thesis Submitted to

The Graduate School of Natural and Applied Sciences of

Ankara Yıldırım Beyazıt University

In Partial Fulfillment of the Requirements for the Degree of Doctor of

Philosophy in Computer Engineering, Department of Computer Engineering

by

Ömer MİNTEMUR

August, 2021

ANKARA

Ph.D. THESIS EXAMINATION RESULT FORM

We have read the thesis entitled "**STEERABLE FILTER IN FREQUENCY DOMAIN WITH ROSE CURVE**" completed by **ÖMER MİNTEMUR** under the supervision of **PROF.DR. FATİH VEHBİ ÇELEBİ** and we certify that in our opinion it is fully adequate, in scope and in quality, as a thesis for the degree of Doctor of Philosophy.

Prof. Dr. Fatih Vehbi ÇELEBİ

Supervisor

Prof. Dr. Recep DEMİRCİ

Jury Member

Asst. Prof. Dr. Osman Serdar GEDİK

Jury Member

Asst. Prof. Dr. Fatih NAR

Jury Member

Asst. Prof. Dr. Duygu SARIKAYA

Jury Member

Prof. Dr. Sadettin ORHAN

Director

Graduate School of Natural and Applied Sciences

ETHICAL DECLARATION

I hereby declare that, in this thesis which has been prepared in accordance with the Thesis Writing Manual of Graduate School of Natural and Applied Sciences,

- All data, information and documents are obtained in the framework of academic and ethical rules,
- All information, documents and assessments are presented in accordance with scientific ethics and morals,
- All the materials that have been utilized are fully cited and referenced,
- No change has been made on the utilized materials,
- All the works presented are original,

and in any contrary case of above statements, I accept to renounce all my legal rights.

Date: **Signature:**

Name & Surname: Ömer Mintemur

ACKNOWLEDGEMENTS

I would like to express my gratitude to my supervisors, both Asst. Prof. Dr. Hilal KAYA and Prof. Dr. Fatih Vehbi ÇELEBİ. They both supported and motivated me endlessly during this study. They pointed me to right direction whenever I was lost. Also, I would like to thank committee member Prof. Dr. Recep DEMİRCİ and Asst. Prof. Dr. Osman Serdar GEDİK who always kindly supported and guided me.

I would also like to thank my roommates İbrahim ATLI, Mahir ŞANLI and Yusuf Şevki GÜNAYDIN for their valuable comments and ideas about the thesis.

Finally, and most importantly, I would like to thank my wife Merve Çolak MİNTEMUR for her support. She always supported me when I was in despair about the thesis. Also, I would like to thank family, my father and mother for their support. This thesis and other achievements in my life would not have been possible without them.

STEERABLE FILTER IN FREQUENCY DOMAIN WITH ROSE CURVE

ABSTRACT

Feature extraction in image processing area is a vital part for further processes in this area. Feature extraction from images is mainly conducted by the filters both in spatial domain and frequency domain. Finding suitable, especially when directional features are in question, in spatial domain is a difficult task. However, feature extraction in frequency domain is more flexible since directions are more obvious in this area. For feature extraction in frequency domain, several methods have been proposed and actively been in use image processing area. One of these methods is Contourlet Transform which does not offer easy direction selectivity. In other words, directions are constant in Contourlet Transform. Another widely used method is 2D Gabor Filter. Although 2D Gabor Filter has flexibility in direction selection, the method suffers from large number of parameters to decide.

In this thesis study, a novel filter for feature extraction in frequency domain using Rose Curve has been proposed. One of the most important properties of the proposed method is angle selectivity. Easiness for the direction selectivity has been achieved by this method. Another property of the proposed method is the number of parameters to decide. The proposed method has only three, easily adjustable parameters. The proposed method has been evaluated on the facial expression classification problem and higher results in terms of different metrics than some of the state of the arts methods in the literature were obtained.

Keywords: Frequency domain, filter, Rose Curve, feature extraction

FREKANS BÖLGESİNDE GÜL EĞRİSİ İLE YÖNLENDİRİLEBİLİR FİLTRE

ÖZ

Görüntü işleme alanında dijital görüntüden özellik çıkarma söz konusu alan için çok önemli bir adımdır. Dijital görüntüden özellik çıkarmak hem uzamsal hem de frekans alanında filtrelerle gerçekleştirilir. Özellikle yön söz konusu olduğunda uzamsal alanda uygun filtreyi bulmak zor bir işlemdir. Ancak, frekans alanında öznitelik çıkarmak, yön kavramı daha belirgin olduğu için çok daha rahat bir alan sağlamasıdır. Frekans alanında görüntüden özellik çıkarmak için literatürde çok sayıda yöntem önerilmiştir. Bunlardan bir tanesi Contourlet Transfrom'dur. Ancak bu metot istenilen yönde kolayca özellik çıkarma özelliğinden yoksundur. Bir başka deyişle, Contourlet Transform'da yönler sabittir. Literatürde sıkça kullanılan diğer bir yöntem ise 2D Gabor Filtresi'dir. Söz konusu filtre frekans alanında yön seçme konusunda esnek olsa da bu metodun karar verilmesi gereken çok sayıda parametresi vardır.

Bu tez çalışmasında, frekans alanında Gül Eğrisi kullanılarak öznitelik çıkaran yeni bir filtre geliştirilmiştir. Geliştirilen metodun en önemli özelliklerinden birisi yön seçimidir. Bu metotla, frekans alanında yön seçiminde kolaylık sağlanmıştır. Önerilen metodun diğer bir özelliği ise parametre sayısıdır. Önerilen metot sadece üç tane, kolayca ayarlanabilir parametreye sahiptir. Önerilen metot, yüzde duygu tanıma sınıflamasında denenmiş olup, literatürde önerilen bazı metotlardan daha üstün sonuçlar elde edilmiştir.

Anahtar Kelimeler: Frekans bölgesi, filtre, Gül Eğrisi, öznitelik çıkarma

NOMENCLATURE

Acronyms

GLCM	Gray Level Co-occurrence Matrix
CNN	Convolutional Neural Network
CT	Contourler Transform
GLT	Gray Level Texture
WCT	Wavelet Coefficient Texture
CCT	Contourlet Coefficient Texture
PCT	Probabilistic Neural Network
BC	Bayer Classifier
IDLP	Ideal Low Pass Filter
GLPF	Gaussian Low Pass Filter
BLPF	Butterworth Low Pass Filter
IDHPF	Ideal High Pass Filter
GHPF	Gaussian High Pass Filter
BHPF	Butterworth High Pass Filter
IBPF	Ideal Band Pass Filter
GBPF	Gaussian Band Pass Filter
BBPF	Butterworth Band Pass Filter
LFT	Lemniscate Filter Type
FER	Facial Expression Recognition
SVM	Support Vector Machine

CONTENTS

LIST OF TABLES

TABLE OF FIGURES

CHAPTER 1

INTRODUCTION

Human eyes can easily interpret an image, or broadly speaking, a scene and derive a meaning from it. It is automatic, moreover, it is an unconscious process for both human eyes and human brain. However, due to rapid development of technology, computers begin to take role in understanding and interpreting images which is called computer vision. But this improvement in technology brings the problem of understanding of images for computers. To give a concrete example, human brain can understand a table from its specific shape. In general, properties of the table, is fixed and processed by human brain automatically. But when it comes to computer vision area, the table's features must be extracted for the computer. Moreover, these features must be meaningful as much as possible such as type of the table, light that comes on to table etc.

Todays, computer vision cover different areas from medical sector to agriculture problems. Advancing in software and hardware systems, many problems once required human power, sliding towards to automatized computer visions solutions. In general, extracted features are used in classification problems, such as detecting disease from an MRI images, face recognition, plant disease classification, by using machine learning algorithms. Features that are not meaningful for a computer will affect the classification results badly.

1.1 Problem Definition and Literature Review

Feature for an image can be described as information contained in it and these information for an image can vary from its color to its shape [1-2]. Moreover, there are other features which can be called as statistical features such as histogram of given image, and Gray-Level-Cooccurrence-Matrix (GLCM) [3-4]. These features can be edges, lines, color, histogram or in general, information that gives overall description of an image. Main meaning of these properties of an image is the necessary part for an image to be understood in light of certain components (edges etc.). Therefore, these features must be

extracted from a given image, and be processed for later usage. This process is called feature extraction. Also, an image itself may contain lots of unnecessary data and these data can be reduced. Thus, another meaning for feature extraction can be given as, changing input into reduced version of it [1]. An example image and its different features given in Figure 1.1.

(a)

(b) (c) (d)

Figure 1.1 An Example Lena Image (a) and Its Distinctive Features (b,c,d)

As can be seen from the Figure 1.1, each part of the image (b,c,d) shows different characteristic feature of the image.

Although, features like histogram and GLCM can contribute to feature extraction process, more features can be extracted based on the image shape. These feature extraction processes are generally based on filters which sometimes called masks [5]. By using filters edges etc. can be extracted visually. These methods can give more concrete features than

statistical features and can be found in literature broadly [6-8]. But these filters work in spatial domain and are slow processes [5]. Moreover, when extracting a feature that lie in a certain direction, extracting that feature requires suitable filter (mask) which can be difficult to construct in spatial domain. In addition, these filters have lack of parametrization in the process of filter creation.

Feature extraction process has been eased by when Convolutional Neural Network (CNN) was proposed [9-10]. CNNs have shown its power in image processing for feature extraction processes [11]. Since CNNs operate by convolving [2] input images with lots of filters, which the filters are learned by the network, directional edges etc. are extracted by filters eventually. Although CNNs are powerful for feature extractors, also it has some drawbacks and solutions of these drawbacks are an active area of research [12-14].

Directional feature extraction in image processing is another active research area. Finding features at desired angle, can enhance the feature extraction process. Since in spatial domain, obtaining desired directional feature is hard, and CNNs have lots of parameters to be optimized, studies have focused on finding directional features on Frequency Domain which is a representation of an image in Fourier Domain [5].

Finding directional features in frequency domain are simpler than in spatial domain or CNNs since frequency domain plane can be divided into horizontal and vertical when edges are concerned. And region between these two axes gives the angled edges or sharp transitions in an image. For these mentioned properties of frequency domain, different filters type has been proposed to extract directional features which can be called steerable filters. Since it is an active area of research many works of steerable filters and their optimizations in frequency domain can be found literature broadly [15-20].

In [21], authors proposed a partition of frequency domain like shape of a checkerboard. Authors used directional filter bank proposed by [19] and further enhanced it for direction selectivity. Authors changed directions proposed by [19] into mini-squares which lie at

different angles, however angles selected by the user cover only small squares thus lots of filters must be prepared.

In [22], authors proposed cascaded directional filter bank for vessel detection. Authors divide frequency partition in 3 stages; however, they use partitioning technique proposed by [19]. In each stage, authors partition frequency plane differently. Since proposed technique is not different from the method in [19], angle selectivity is still constrained. In [23], authors add direction selectivity property to normal wavelet transforms. However proposed method is mathematically complex and there are some constraints mentioned by the authors.

In [24], authors mentioned that before applying normal directional partition in frequency domain, DC component must be removed. Thus, authors proposed different versions of usual directional partition of the frequency domain proposed by [19]. Authors changed number of directions (normally 8 subbands is considered) in their work to 6 directional subbands. However, partition of the frequency domain is not different from the work in [19].

Authors in [25] reduced the complexity of directional filters in their work, however partition logic is still the same as before. In [26], authors proposed a derivative of usual directional partition of the frequency domain. Main idea of the proposed technique is passing results of wavelet filters through a filter bank. Purpose of this process is to enhance the wavelet results. However, since authors uses the usual partition of directional filter bank, desired features lie at different angles cannot be enhanced easily.

Usual partition proposed by [19] does not cover fully both horizontal and vertical portions of frequency domain. To solve this problem, authors in [27] proposed a new directional partition of frequency domain. Work in mentioned study increases the number of directions and by doing this, their method fully covers the horizontal and vertical portions

of the frequency domain. However, same problem holds which is limited number of directions.

In general partition of frequency domain is conducted in 2D, however in [28], authors enhanced usual partition of frequency domain to 3D (authors mentioned their method works in when dimension is bigger than 2) domain.

Further studies concerning steerable filter in frequency domain also proposed different versions for partitioning of the frequency domain [29-30]. In general, proposed filter have lack of parameter selection and they are not easily modifiable. These filters' type is generally diamond shaped, called wedge (Figure 1.2), and covers only the certain parts of frequency domain and, when steering is in question, steering ability of these filters are limited.

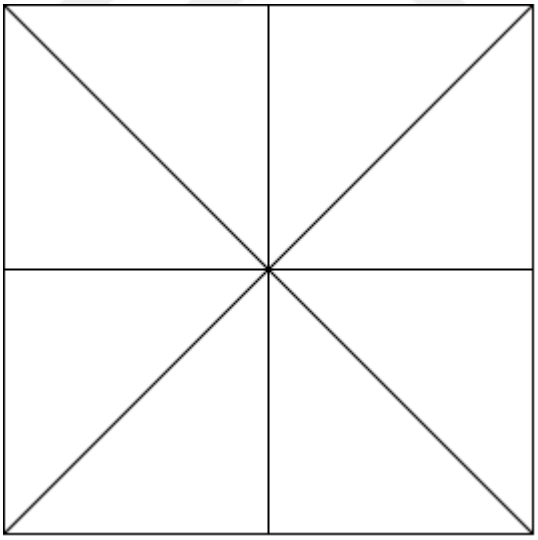

Figure 1.2 Example Division of Frequency Domain

One popular version of steerable filters is Contourlet Transform (CT) [31]. It was proposed in 2005 as an extension of Wavelet Transform [32]. Contourlet Transform overcomes the problem of directionality in Wavelet Transform. Wavelet Transform extracts feature only horizontally, vertically and diagonally in an image. However,

Contourlet Transform divides frequency plane into many more directions. This flexibility of Contourlet Transform has been used in many applications in literature. As its field of usage varies, i.e., CT finds its usage in classification [33-45], image fusion [46 – 54], image reconstruction [55-56], denoising [57-64], image retrieval [65], watermark detector-embedding [66-68].

To give specific examples about how CT is used for feature extraction, in [69], authors diagnose liver tumors on CT images. Authors divide their automation system into three parts. First, authors automatically extract tumor using Alternative Fuzzy c-means (AFCM) clustering to extract the tumor. Second stage of the automation process is feature extraction process which contains Gray Level Texture (GLT) Features, Wavelet Coefficient Texture (WCT) and Contourlet Coefficient Texture (CCT). Then authors extract different sub features from these features. Finally, extracted features fed into Probabilistic Neural Network (PNN). In [70], authors classify textures using CT. Authors used three level decomposition of CT and extract coefficients, in other words, features. Then differences between these features are calculated for the defect detection. And these differences were fed into Bayes Classifier (BC) for classification.

However, CT only extracts certain parts of frequency domain, and works in the literature rely on certain feature extraction patterns (4 subbands, 8 subbands etc.). In addition, CT has no flexibility when parameters are in question. Thus, this brings the parameter selection problem for CT since there are no certain rules for selecting parameters in CT. Another issue for CT is that only one direction can be selected in one filter.

Another popular steerable filter used in literature is 2D Gabor Filter [71]. This filter is very popular since it can capture edges and lines of a given image. Generally, to extract different features from a given image, a filter bank is constructed with different parameter values of 2D Gabor Filter. The most important property of 2D Gabor Filter is the selection of angle. By selecting desired angle, a steerable filter can be prepared. In general, process of feature extraction is similar to CT. Firstly, a set of filters are prepared using 2D Gabor

Filter parameters, then these prepared filters are applied to the image and features are extracted. Then these features are generally fed into a machine learning algorithm. Like CT, 2D Gabor Filter has been used in the literature broadly [72-81] and finds its usage for classification problems.

In [82], authors used 2D Gabor Filter and Adaboost Classifier to classify the facial expressions. However, as authors mentioned, 40 different filters are prepared with 8 directions and 5 scales. Authors also employed another algorithm to select the discriminative features of the prepared feature vector. However, parameters of 2D Gabor Filter were needed to be decided and lots of filter was prepared in this work.

In [83], another work that uses 2D Gabor Filter is presented. Authors prepared 40 different filters with different parameters. Authors divided the face images into four parts (two eye parts, one mouth and one lip) and filtered this part with the prepared filters. Again, lots of filters had to be prepared and although Principal Component Analysis (PCA) was used, feature vector dimension was relatively high. Study in [84], focuses only lips and eyes after filtering faces with 40 different 2D Gabor Filter. After filtering process, eyes part and lips part are extracted, and LBP was used for further feature extraction process.

Although 2D Gabor Filter works in spatial domain, this filter also has a response in frequency domain. Each prepared filter corresponds certain part of frequency domain, since only certain part covered, lots of filters must be prepared. Moreover, filter preparation process in 2D Gabor Filter is a complex process since 2D Gabor Filter has 6 parameters to be decided by the user. And each parameter has its own restriction. As number of filters increase, complexity of the work increases.

1.2 Aim of the Thesis

By taking into considerations these limitations mentioned in section 1.1, a filter which is fully modifiable, use less parameters than the proposed methods in the literature, constraint free in direction selection is to be a great contribution to this area. Thus, in this thesis, this kind of filter is proposed using Rose Curve.

Also, selection of more than one direction by this proposed filter would ease feature extraction process. Finally, combination of different filters with this proposed steerable filter also could be a great contribution to the literature.

The proposed filter is a new filter in the literature and was used in a facial expression classification problem in this thesis, and results of the experiments were compared with the existing solutions in the literature.

1.3 Structure of the Thesis

The paper is organized in the following manner: Chapter 2 presents Fourier Transform and filtering technique in Fourier Transform. Chapter 3 gives details about CT and 2D Gabor Filter. Chapter 4 presents the proposed method for steerable filter in frequency domain using Rose Curve. In chapter 5 Rose Curve filter is used on the classification of facial expression based on CK48+ dataset and gives experimental results which surpasses some of the state-of-art methods. Chapter 6 draws conclusions reached from study. Finally, Chapter 6 discuses about the presented study and future works.

CHAPTER 2

DIGITAL IMAGE PROCESSING AND FOURIER DOMAIN FILTERING

2.1 Image Definition

By using some analogy, one can define the image as a scene captured by a human eye or a camera. After capturing the scene, the captured scene must be transformed to some data structure, mainly to a matrix. This process is called image digitization. Image digitization means that the image function $f(x,y)$ is sampled and turned into a matrix which has M rows and N columns. An integer is assigned to each pixel in the coordinate of $f(x,y)$ which is called image quantization. Quality of the sampling and quantization determines the image resolution. Although sound simple, quantization can be a problem when image processing is in question. If insufficient brightness level in quantization process is used, image quality drops significantly. In other terms, quantization can be thought as bit-level of images. If 256 brightness level is used, image is called 8-bit image. That means that every pixel in the image has value between 0 – 255. 0 is black, and 255 is white. A sample image in $x-y$ plane is given in Figure 2.1.

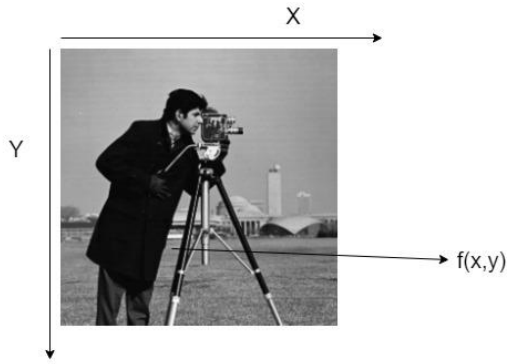

Figure 2.1 Sample Image Coordinate System

A digital image consists finite number of pixels, and each pixel has a location and value. As grayscale images have value between 0 – 255. colorful images have three difference channel namely red channel, green channel, and blue channel and it has value between 0-255 for each channel. Combination of these three channels gives the colorful image. An example colorful image's decomposition into three channels is given in Figure 2.2.

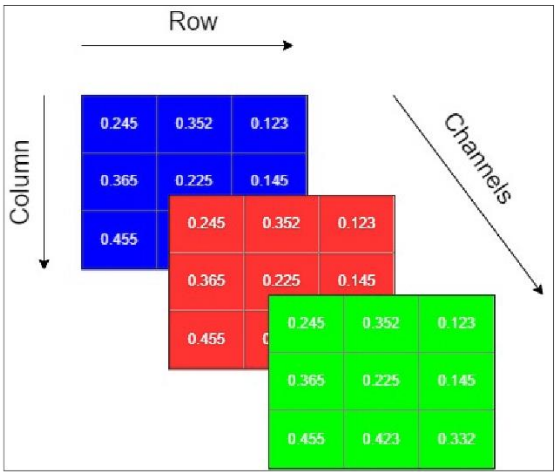

Figure 2.2 Simple Decomposition of Colorful Image

Colorful images are constructed as combination of values in each channel. To give an example when values of each channel is to be (255, 255, 255), resultant image will be white whereas black color will (0, 0, 0).

2.2 Image Filtering

In general, images are not used directly in image processing. Thus, some further modifications are needed. These modifications can be achieved by a filter. Filtering term originally used for frequency domain, which means passing or rejecting specific frequency coefficient of the given image. However, filtering process can be done also in spatial domain in image processing area. For both domains, filtering term yields to modification of image pixel values or frequency coefficients. Main purpose of the image filtering whether done in spatial domain or frequency domain is to extract valuable information, called feature, from the given image. Generally, a filter is defined by a kernel which is a square matrix that has odd size (3,5,7, etc.). In spatial domain, filtering can be achieved by a technique called convolution. A simple convolution process in spatial domain is given in Figure 2.3.

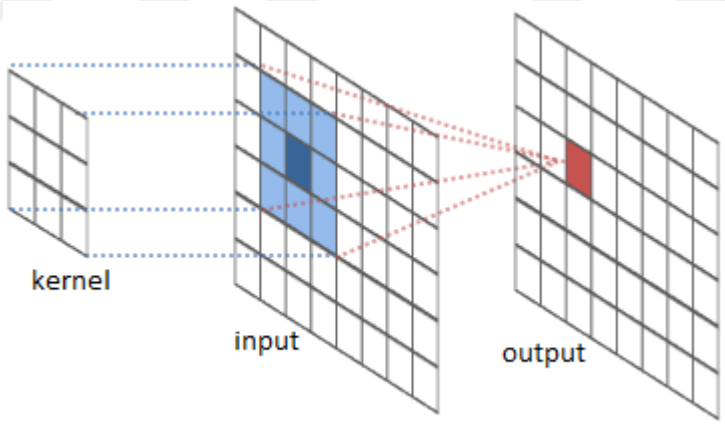

Figure 2.3 Simple Filtering in Spatial Domain [85]

Generally, filtering in spatial domain is slow and finding a proper mask for the desired process may be overwhelming. However, in frequency domain filtering can be done simply by multiplying the image in frequency domain by a kernel. This method is faster than filtering in spatial domain, since in frequency domain, filtering is a simple multiplication. Next section will introduce the Fourier Domain in image processing area and mention fundamental filtering methods in this domain.

2.3 Fourier Transform

In 1822, Joseph Fourier showed that any waveform can be represented as sum of sine and cosine functions and developed a transform which has been used since that time. In general, Fourier Transform transforms any waveform to its alternative form. Usage of Fourier Transform can be seen in many areas, some of them are signal and image processing and quantum mechanics [86]. Since images are considered in this context, Fourier Transform in image processing, particularly Discrete Fourier Transform (Eq 2.1), is considered.

$$F(u,v) = \sum_{x=0}^{M-1} \sum_{y=0}^{N-1} f(x,y) e^{-2i\pi(\frac{ux}{M} + \frac{vy}{N})} \quad \textbf{(2.1)}$$

Where M represents the row number, N represents the column number. Images are generally represented in spatial domain, however another form of representation of images are in frequency domain. An example image of both spatial domain and Fourier domain is given in Figure 2.4.

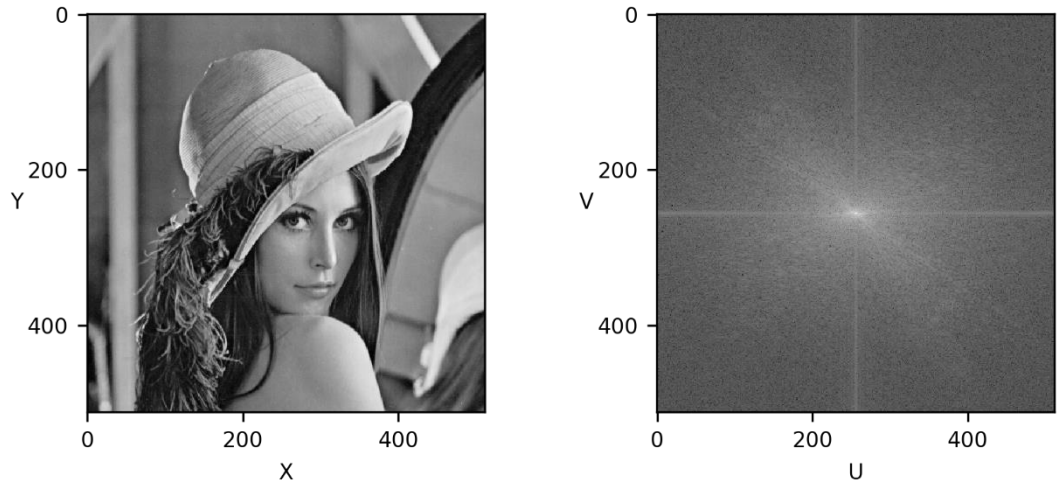

(a) (b)

Figure 2.4 (a) Image in Spatial Domain, (b) Image in Fourier Domain

Some of the motivations that has given rise to use Fourier Transform in image processing is that, in spatial domain some of the image features are not visible, by transforming into frequency domain, these features can be extracted. Another motivation is filtering processing can be done faster in Fourier domain than in spatial domain. In spatial domain, x-y coordinates represent the intensity value (a real valued number) of the image. However, in frequency domain x-y value of the given image represents its frequency and amplitude. In this domain, x-y corresponds the frequency and its value correspond the amplitude. In other words, at each coordinate in frequency domain shows us how much the harmonic frequency component contributes to the image. When the transformation is applied, the given image is basically divided into two main parts, namely, high frequencies and low frequencies (See Figure 2.5). However, a strict line cannot be drawn between low frequencies and high frequencies in Fourier domain. In Figure 2.5, bigger circle radius means higher frequencies in Fourier domain.

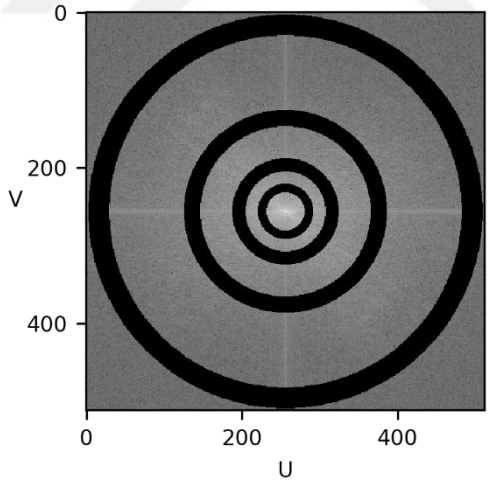

Figure 2.5 As Circle Gets Bigger Higher Frequencies Can be Obtained

After filtering operation done in Fourier domain, by using Inverse Fourier Transform (Eq 2.2), image can be recovered to spatial domain.

$$f(x,y) = \frac{1}{MN}\sum_{u=0}^{M-1}\sum_{v=0}^{N-1} F(u,v) e^{2i\pi\left(\frac{ux}{M}+\frac{vy}{N}\right)} \qquad \textbf{(2.2)}$$

2.4 Frequency Domain Filtering Types

Filtering in frequency domain is a very straight process. Image is transformed into Fourier domain, multiplied with a filter and the Inverse Fourier Transform is applied to image (Eq 2.3).

$$g(x,y) = \text{Real}\{F^{-1}[H(u,v)F(u,v)]\} \quad \textbf{(2.3)}$$

where F^{-1} is the Inverse Fourier Transform, $F(u,v)$ is the Fourier Transform of the given image, $H(u,v)$ is the filtering function. In this equation $F(u,v)$ and $H(u,v)$ must have the same size. Also, in this equation $H(u,v)$ must be symmetric about their origin which simplifies the operation.

The main point of filtering is to decide which frequency band to pass and which frequency band to be suppressed. A filter can be characterized by three parameters in general: *Distance function, Cut-off frequency,* and *band-with.*

Distance Function: If a transfer function is to be generated as distance of each element from the origin, distance in the transfer function is needed to be known. In transfer functions, the distance is generally denoted as $D(u,v)$ or simply denoted as D.

Cut - off Frequency: This parameter is to decide where (as a distance) a filter stops or allows to pass the frequency bands. It is denoted as D_0.

Band – Width: This parameter can be used in band – reject or band – pass filters. It is a distance that deciding between lower and upper cutoff frequencies which are either rejected or passed.

Filters in frequency domain can be divided into two parts, low pass filters which consist filters that allow low frequencies passing and high pass filters that allow high frequencies passing. Next two subsections will introduce these filtering types.

2.5 Low Pass Filters (Smoothing Filters)

In Fourier domain, high frequencies correspond to sharp transitions, edges etc. Therefore, when a low pass filter is to be designed, high frequency components of the given image is attenuated, and low frequencies remain unchanged. This process brings out the general shape of the given image since and edges and sharp transitions are attenuated.

2.5.1 Ideal Low Pass Filter (Smoothing Filter)

This filter type is the most common and most simple filter type. The ideal low pass filter (IDLPF) attenuates all frequencies higher than the cut-off frequency D_0. Typical formula of the IDLPF is given in Equation 2.4.

$$H(u,v) = \begin{cases} 1 & if \quad D(u,v) \le D_0 \\ 0 & if \quad D(u,v) \ge D_0 \end{cases} \tag{2.4}$$

where D_0 is the cut off frequency $D(u,v)$ is the distance function. $D(u,v)$ for an image which has a size of $M\ x\ N$ can be described as;

$$D(u,v) = \sqrt{(u - \frac{M}{2})^2 + (v - \frac{N}{2})^2} \tag{2.5}$$

An IDLP is radially symmetric about the origin. An example of IDLP in frequency domain can be seen in Figure 2.6.

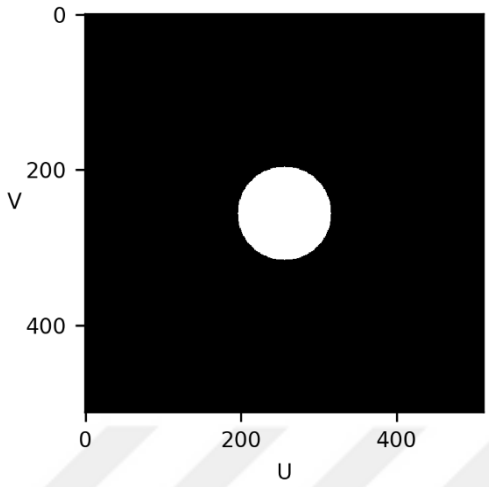

Figure 2.6 An Ideal Low Pass Filter – $D_0 = 60$.

In Figure 2.6 U axis represents the vertical edges in spatial domain, and V axis represents the horizontal axis in spatial domain. In other words, if frequencies along the U axis is to be extracted, vertical edges in can be seen in spatial domain, however if frequencies along the V axis, horizontal edges can be seen in spatial domain.

Results of ideal low pass filter for different cut-off frequencies can be seen in Figure 2.7. Since high frequency components of the image is attenuated, the image is blurred. As cut-off frequency becomes higher, more frequencies are allowed. Thus, image does not change dramatically. However, one main drawback of the ideal low pass filter is ringing effect [5]. This effect, results of sharp transition between border of the cut-off frequency. The effect can be more severe as D_0 decreases.

(a)

(b) (c) (d)

Figure 2.7 (a) Original Lena Image (512x512). (b) D_0 = 30 (c) D_0 = 60 (d) D_0 = 90

When D_0 becomes larger, more frequency components of the image are passed, thus image is recovered almost perfectly. But when D_0 becomes smaller, less frequency components of the image are passed; thus, image is blurred. Figure 2.7 (a) shows the original, not filtered Lena image. Figure 2.7 (b) shows the Lena image filtered with low pass filter ($D_0 = 30$). Since radius is small, image was slightly distorted. However, as radius is getting bigger, distortion was reduced as can be seen in Figure 2.7 (c,d).

2.5.2 Gaussian Low Pass Filter (Smoothing Filter)

Gaussian Low Pass Filter (GLPF) is another important filter type in image processing area. Typical GLPF formula is given in Equation 2.6.

$$H(u,v) = e^{-D(u,v)^2/2D_0^2} \quad \textbf{(2.6)}$$

where, like IDLP, D_0 controls the cut-off frequency. The most important property of GLPF is that the filter does not produce ringing effect in filtered image. Figure of GLPF in frequency domain is given in Figure 2.8 and results of GLPF for different cut-off frequencies is given in Figure 2.9 respectively.

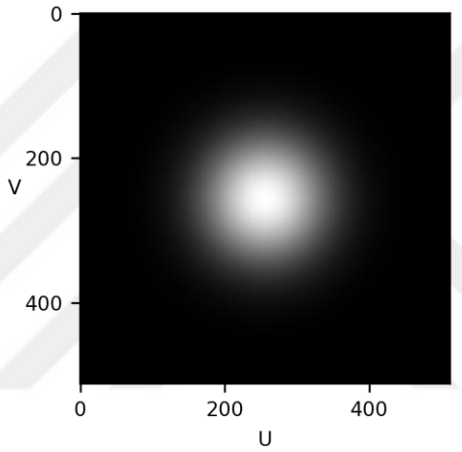

Figure 2.8 A Gaussian Low Pass Filter – $D_0 = 60$

(a)

(b) (c) (d)

Figure 2.9 (a) Original Lena Image (512x512). (b) D_0 = 30 (c) D_0 = 60 (d) D_0 = 90

2.5.3 Butterworth Low Pass Filter (Smoothing Filter)

Another commonly used filtering type is Butterworth Low Pass Filter (BLPF). This filter is similar to GLPF. Transfer function $H(u,v)$ of Butterworth filter is given in Equation 2.7.

$$H(u,v) = \frac{1}{1+\left[\frac{D(u,v)}{D_0}\right]^{2n}} \qquad \textbf{(2.7)}$$

where n is the order of BLPF, D_0 is the cut-off frequency. This filter type differs from other low pass filter types in terms of parameter n. This parameter controls the filter's behavior. As n increases, the BLPF behaves like IDLP. Effect of the parameter n for the BLPF can be seen in Figure 2.10. In Figure 2.10, each filter's D_0 was selected as 60. Also results of BLPF for different cut-off frequencies (the parameter n is constant) is given in Figure 2.11.

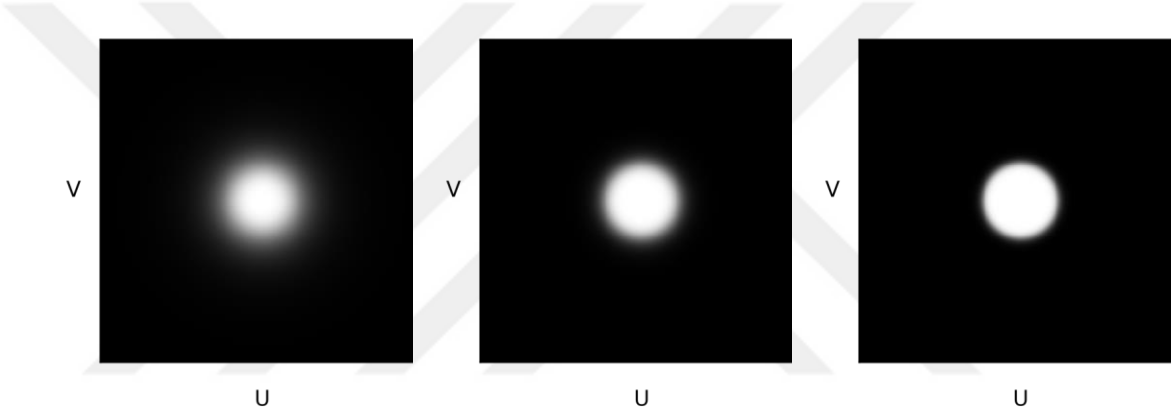

(a) (b) (c)

Figure 2.10 BLPF Filter Behavior as n Changes (D_0 = 60 for all). (a) n = 2, (b) n = 4, (c) n = 8.

As can be seen Figure 2.10, when order of the Butterworth is getting bigger, the filter behaves like IDLPF. In Figure 2.10 (a) the order was selected as 2, and the filter is similar to GHPF, however, in Figure 2.10 (c) the order was selected as 8, and the filter is more similar to IDLPF.

(a)

(b) (c) (d)

Figure 2.11 (a) Original Lena Image (512x512). (b) D_0 = 30 - n = 2 (c) D_0 = 60 - n = 2 (d) D_0 = 90 - n = 2

In Figure 2.11 (b,c,d), the order of the Butterworth filter was kept constant. However, radius was changed as 30, 60, 90. When the order selected as 2, the filter acts similar to GHPF as mentioned above.

2.6 Sharpening Filters (High Pass Filters)

Sharpening filters in frequency domain reveals the edges in the image. Thus, these types of filters are used to extract edges and sharp transitions. Similar to low pass filters, a high pass filter blocks out the certain frequency components and allows other frequency components passing. High pass filters are the inverse of low pass filters. In general, there

are three types of high pass filters in frequency domain. This section explains these filters, namely Ideal High Pass Filter (IDHPF), Gaussian High Pass Filter (GHPF) and Butterworth High Pass Filter (BHPF)

2.6.1 Ideal High Pass Filter (Sharpening Filters)

IDHPF is the inverse of an IDLPF, and its formula is given in Equation 2.8.

$$H(u,v)_{HP} = 1 - H(u,v)_{LP} \quad \textbf{(2.8)}$$

where $H(u,v)_{LP}$ is the same equation which was given in Equation 2.4. An IDHPF is given in Figure 2.12.

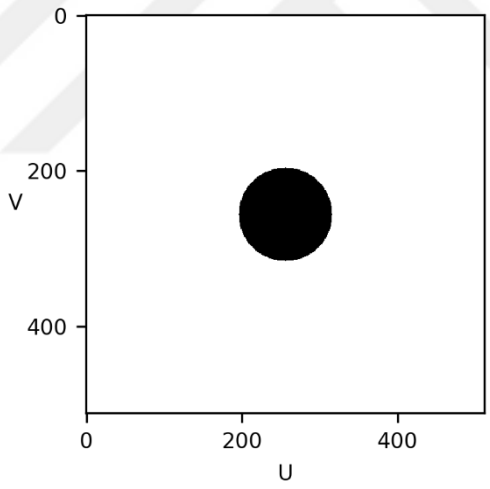

Figure 2.12 - An Ideal High Pass Filter – D_0 = 60

In Figure 2.13, results of IDHPF can be seen. All Ideal filter types, whether low pass or high pass suffer from ringing effect. This effect can be seen clearly (especially Figure 2.13 (b)) as cut-off frequency decreases.

(a)

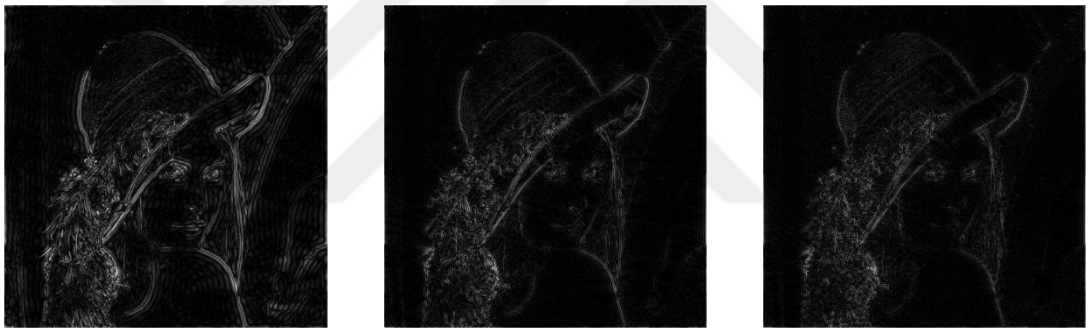

(b) (c) (d)

Figure 2.13 (a) Original Lena Image (512x512). (b) $D_0 = 30$ (c) $D_0 = 60$ (d) $D_0 = 90$

As can be seen from the Figure 2.13, sharper edges can be extracted as radius increases. In Figure 2.13 (b), since radius is small relative to Figure 2.13 (c, d) more frequencies was allowed. Thus, general edges of the Lena image were extracted. However, as radius is getting bigger (Figure 2.13 (d)), sharper edges was extracted.

2.6.2 Gaussian High Pass Filter (Sharpening Filters)

Transfer function of GHPF is given in Equation 2.9.

$$H(u,v)_{GHPF} = 1 - H(u,v)_{GLPF} \quad \textbf{(2.9)}$$

where $H(u,v)_{GLPF}$ is the equation given in Equation 2.7. GHPF does not suffer from ringing effect as mentioned in section 2.5.2. An example GHPF is given in Figure 2.14. Also results of GHPF are given in Figure 2.15.

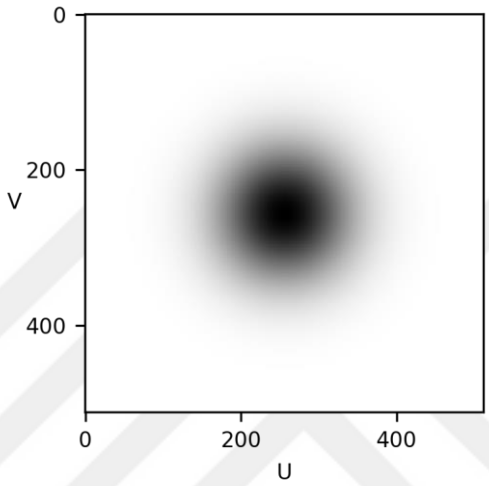

Figure 2.14 A Gaussian High Pass Filter – $D_0 = 60$

(a)

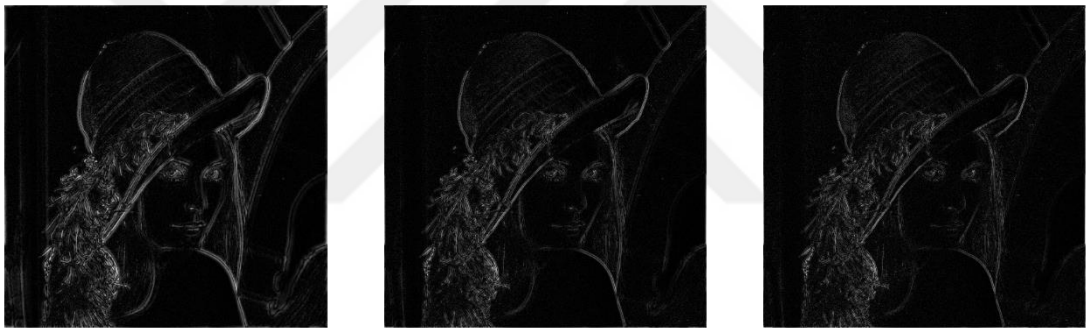

(b) (c) (d)

Figure 2.15 (a) Original Lena Image (512x512). (b) D_0 = 30 (c) D_0 = 60 (d) D_0 = 90

Main difference between IDHPF and GHPF is ringing effect. This effect can be seen in Figure 2.15 clearly. Especially Figure 2.15 (b) and Figure 2.13 (b) show the difference between these two filters. As radius is getting bigger, higher frequencies, sharper edges in spatial domain, can be extracted similar to IHPF. However, this time ringing effect is eliminated.

2.6.3 Butterworth High Pass Filter (Sharpening Filters)

Transfer function of BHPF is given in Equation 2.10.

$$H(u,v)_{BHPF} = 1 - H(u,v)_{BLPF} \quad \textbf{(2.10)}$$

where $H(u,v)_{BLPF}$ is the equation given in Equation 2.6. An example GHPF is given in Figure 15. Also results of BHPF is given in Figure 2.16.

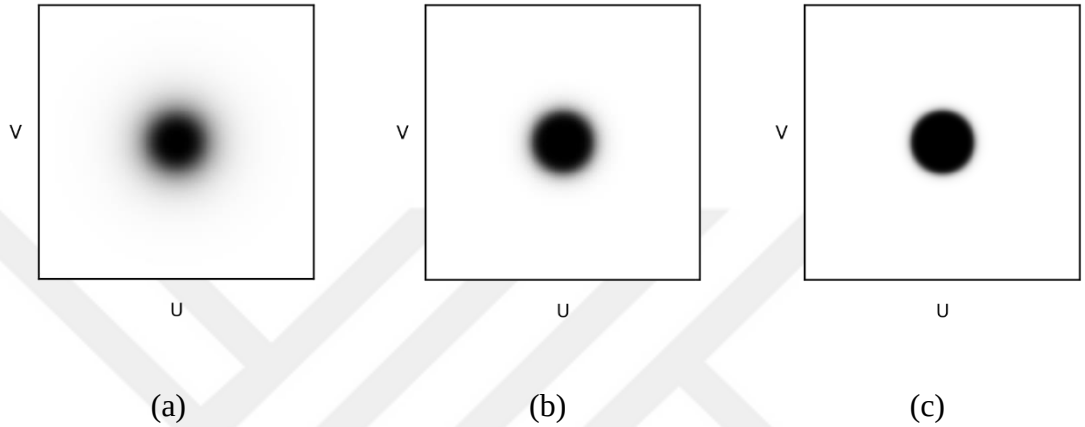

Figure 2.16 BHPF Filter Behavior as n Changes (D_0= 60 for all). (a) n = 2, (b) n = 4, (c) n = 8.

(a)

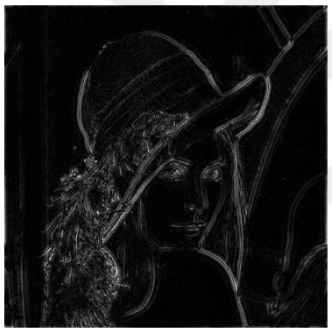

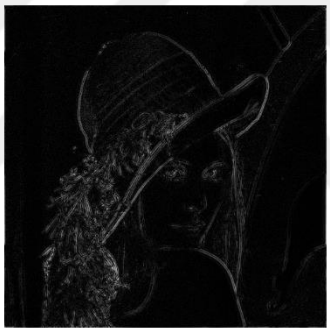

(b) (c) (d)

Figure 2.17 (a) Original Lena Image (512x512). (b) $D_0 = 30$ - n = 2 (c) $D_0 = 60$ - n = 2 (d) $D_0 = 90$ - n = 2

As can be seen from the Figure 2.17, BHPF behaves like GHPF when the order is small. In Figure 2.17 (a) radius was selected as 30 and general edges were extracted. However, as radius is getting bigger sharper edges can be extracted.

2.7 Band Pass Filters

Filters have been discussed until now, work over entire frequency domain. However, some applications may need some parts of the frequency domain to be passed and some parts of the frequency domain not to be passed. These filters are called band-pass filters. Band-pass filters can be divided into three groups namely, Ideal Band Pass Filters (IBPF), Gaussian (GBPF) and Butterworth (BBPF).

2.7.1 Ideal Band Pass Filters

Ideal band-pass filter acts like IDHPF and IDLPF filters. Only difference is that this filter passes frequency at certain range, other frequencies are attenuated. IBPF's formula is given in Equation 2.11. An example of IBPF and its result is given in Figure 2.18 and Figure 2.19 respectively.

$$H(u,v) = \begin{cases} 0 & \text{if} \quad D_0 - \frac{W}{2} \le D(u,v) \le D_0 + \frac{W}{2} \\ 1 & \text{otherwise} \end{cases} \tag{2.11}$$

where, D_0 is the cut-off frequency W is the width of the band.

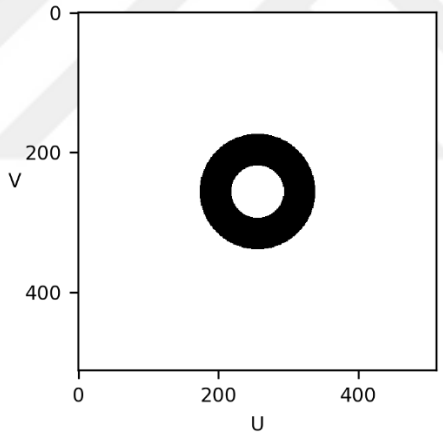

Figure 2.18 An Ideal Band Pass Filter. W = 45, D_0 = 60

(a)

(b) (c) (d)

Figure 2.19 (a) Original Lena Image (512x512). (b) D_0 = 60 - W = 15. (c) D_0 = 60 - W = 30. (d) D_0 = 60 - W = 45.

2.7.2 Gaussian Band Pass Filters

GBPF's formula is given in Equation 2.12. Example of GPBF and its results for different values for D_0 and W is given in Figure 2.20.

$$H(u,v) = 1 - e^{-\left[\frac{D(u,v)^2 - D_0^2}{D(u,v)W}\right]^2} \quad \textbf{(2.12)}$$

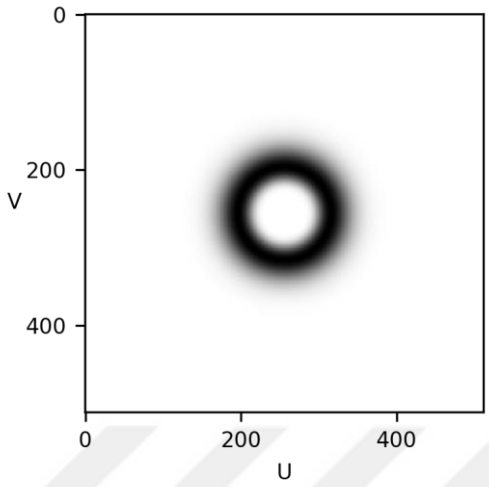

Figure 2.20 A Gaussian Band Pass Filter. W = 45, D_0 = 60

(a)

(b) (c) (d)

Figure 2.21 (a) Original Lena Image (512x512). (b) D_0 = 60 - W = 15. (c) D_0 = 60 - W = 30. (d) D_0 = 60 - W = 45.

2.7.3 Butterworth Band Pass Filters

BBPF's formula is given in Equation 2.13, where n is the order of Butterworth Filter. Example of BBPF and its results applied on Lena image are given in Figure 2.22 and Figure 2.23 respectively.

$$H(u,v) = \frac{1}{1+\left[\frac{D(u,v)W}{D(u,v)^2 - D_0^2}\right]^{2n}} \quad \textbf{(2.13)}$$

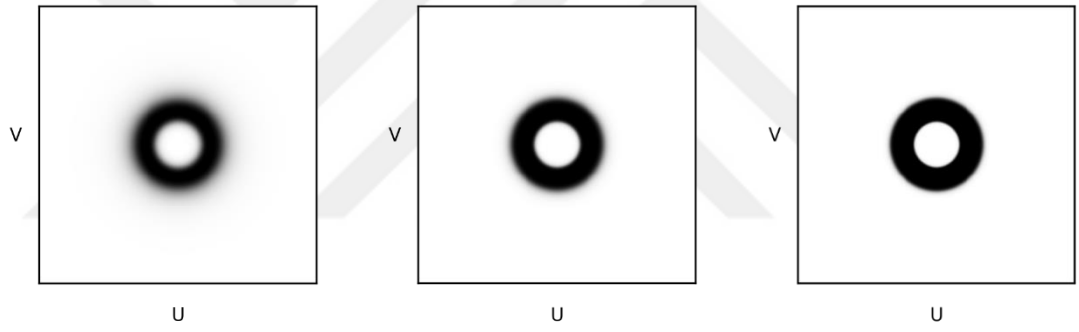

(a) (b) (c)

Figure 2.22 BBPF Filter Behavior as n Changes (D_0= 60 for all). (a) n = 2, (b) n = 4, (c) n = 8.

(a)

(b) (c) (d)

Figure 2.23 (a) Original Lena Image (512x512) (n=2 for All). (b) D_0 = 60 - W = 15. (c) D_0 = 60 - W = 30 (d) D_0 = 60 - W = 45.

2.8 Comments on Presented Filters

Filters which have been presented in this section can find its place in the literature differently. Low pass filters can be used to detect visual saliency [87], band pass filters can be used in image denoising [88] and high pass filters [89] can be used for feature extraction. However, all filters presented in this section do not have direction selectivity. Filters in this section span all angles in frequency domain because of their shape. Only parameter can be controlled for low pass and high pass filters is cut-off frequency. For band-pass filters, cut-off frequency and band width can be controlled. In some applications, extracting certain directions in frequency domain is important and this ability of any filter provides user to extract any directional information desired, not the whole information.

For these reasons, works that have been conducted for extracting directional information in frequency domain has been presented. Next section mentions two of the most used filter types for extraction directional information namely 2D Gabor Filter and Contourlet Transform.

CHAPTER 3

STEERABLE FILTERS

Typically, steerable filters can be defined as the filters that are able to extract directional edges in an image. Historically, [90] showed that in spatial domain steering property can be achieved by manipulating Gaussian filter. However, this filter was conducted on spatial domain, and for each direction, a derivative of Gaussian function is needed.

Another proposed method for a steerable filter works in frequency domain proposed by [19]. Proposed method is based on partition of frequency domain in each direction. Methods mentioned in the Introduction section mainly was about this partition technique. In this section of the thesis, two of the most used methods in the literature for steerable filters is mentioned. First, 2D Gabor Filter is presented which works on both spatial domain and frequency domain. Another method which is mentioned in this section is Contourlet Transform proposed by [31]. The method basically relies on partition technique proposed by [19]. Main difference proposed by the authors is a high pass property placed on middle of the frequency domain to extract high frequencies.

3.1 2D Gabor Filters

2D Gabor Filter proposed by Daugman [71] in 1980 on top of 1D Gabor function. This filter type is a product of Gaussian function which is elliptic and complex exponential function which represents sinusoidal plane. 2D Gabor Filter can be defined as:

$$g(x, y, f, \theta) = e^{-\frac{1}{2}\left[\frac{x_\theta^2}{\sigma_x^2}+\frac{y_\theta^2}{\sigma_y^2}\right]}.e^{j2\pi f x_\theta} \quad \textbf{(3.1)}$$

where f is the frequency of the sinusoidal plane, θ is the orientation of the Gabor Filter. σ_x is the sharpness along x axis and σ_y is the sharpness along the y axis. Finally, x_θ and y_θ can be defined as:

$$x_\theta = x\cos(\theta) + y\sin(\theta) \quad \textbf{(3.2)}$$

$$y_\theta = -x\sin(\theta) + y\cos(\theta) \quad \textbf{(3.3)}$$

Most applications use real part of Equation 3.1. Thus, formula of the 2D Gabor Filter becomes:

$$g(x, y, f, \theta) = e^{-\frac{1}{2}\left[\frac{x_\theta^2}{\sigma_x^2} + \frac{y_\theta^2}{\sigma_y^2}\right]}.\cos(2\pi f x_\theta) \quad \textbf{(3.4)}$$

Another common formula which used in this thesis is given in Equation 3.5.

$$g(x, y; \lambda, \theta, \psi, \sigma, \gamma) = \exp\left(-\frac{x'^2 + \gamma y'^2}{2\sigma^2}\right)\exp\left(i\left(2\pi\frac{x'}{\lambda} + \psi\right)\right) \quad \textbf{(3.5)}$$

where λ is the wavelength of the sinusoidal, θ is the orientation, ψ is the phase offset, σ is the standard deviation of the Gaussian envelope, and lastly γ determines the ellipticity of the Gabor Function. x' and y' are the same as Equation 3.2 and 3.3 respectively. Gabor Filter normally works in spatial domain, which means a convolution process is applied to an image that is being filtered. But each Gabor Filter that is prepared using the parameters has equivalent frequency domain response. A simple 2D Gabor Filter's response in each domain is given in Figure 3.1.

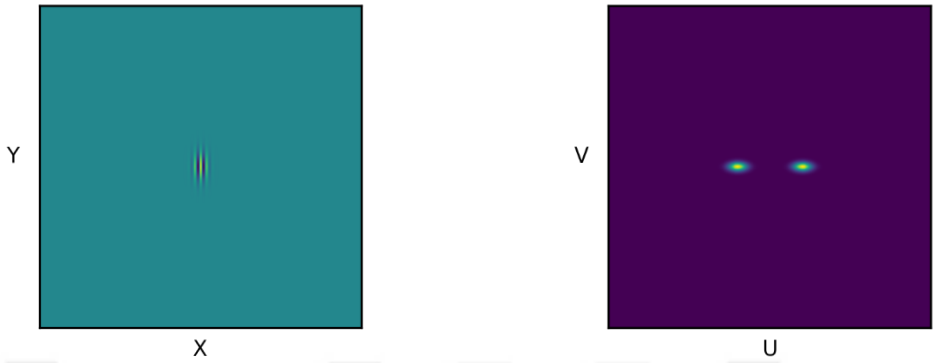

Figure 3.1 2D Gabor Filter Example. (a) Spatial Domain, (b) Frequency Domain

Parameters:λ=10, θ=π, ψ=0, σ=8.0, γ=0.5

Since thesis's main domain is frequency domain, from Figure 3.1, it can be easily deduced that, more than one filter must be prepared to cover all areas of the frequency domain. And for each filter 6 different parameters must be decided. As a result, a filter bank can be constructed. An example of filter bank constructed with 2D Gabor Filter in frequency domain is given in Figure 3.2.

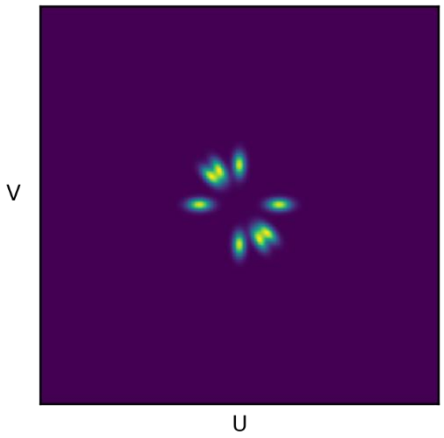

Figure 3.2 A 2D Gabor Filter Bank Example

Parameters: λ=10, θ=(π,π/2,π/3,π/4) ψ=0, σ=8.0, γ=0.5, ksize=512x512

When 2D Gabor Filter Bank is considered (Figure 3.2), it is not possible to capture whole frequencies lies at certain angle. Thus, lots of filter must be prepared. This process may not be feasible always. An example of filtered image with the filter bank given in Figure 3.2 is given in Figure 3.3.

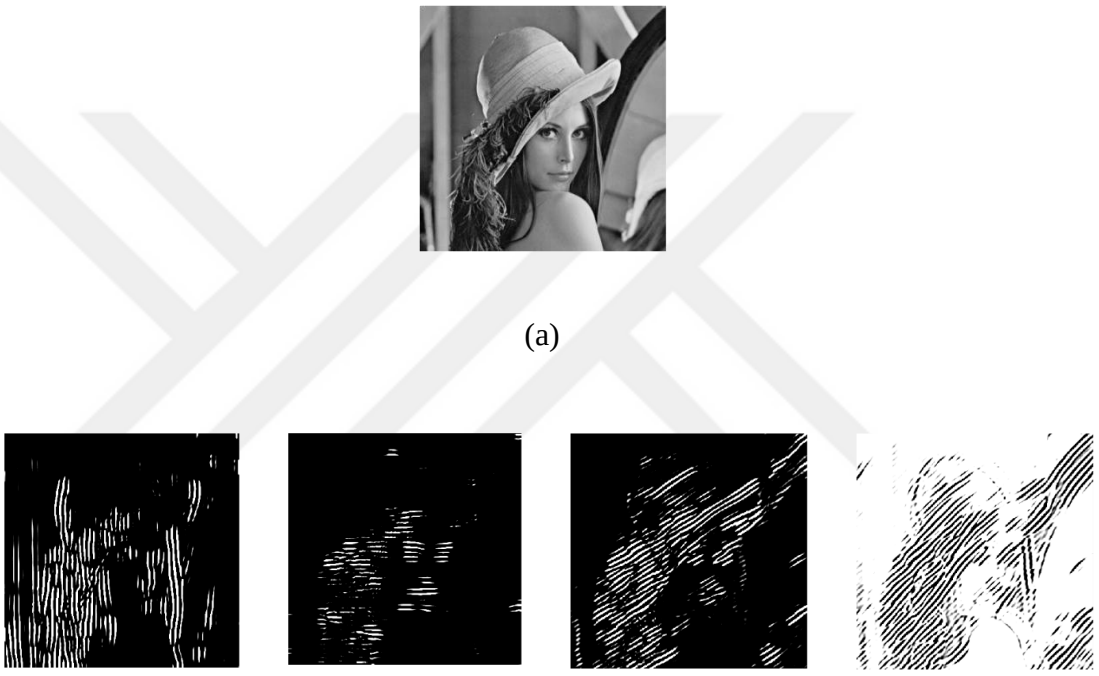

(a) (b) (c) (d) (e)

Figure 3.3 Results of 2D Gabor Filter Bank. (a) Original Image. (b) (c) (d) (e) Results

Parameters: λ=10, θ=(π(a),π/2(b),π/3(c),π/4(d)) ψ=0, σ=8.0, γ=0.5, ksize=32x32

Figure 3.3 gives some insights about 2D Gabor Filter. Since the filter does not fully covers frequency domain, filtered images are lack of full description. For example, in Figure 3.2 (b) horizontal features of Lena image is extracted. However, due to the mentioned problem above, not all horizontal features were extracted. These problems can be said for all other three images (Figure 3.2 (c,d,e)). For these reasons all parameters of 2D Gabor Filter must be decided carefully to extract decent features from the given image.

Beside mentioned issues, 2D Gabor Filter has some limitations when deciding parameters [74]. As expected, θ should be between 0 and 2π. In general, λ is set to be bigger than 2. ψ must be between -π and π. Aspect ratio γ must be between 0 and 1.

3.2 Contourlet Transform

Contourlet Transform is basically based on frequency partition technique proposed by [19]. Schema proposed by the authors is given in Figure 3.4.

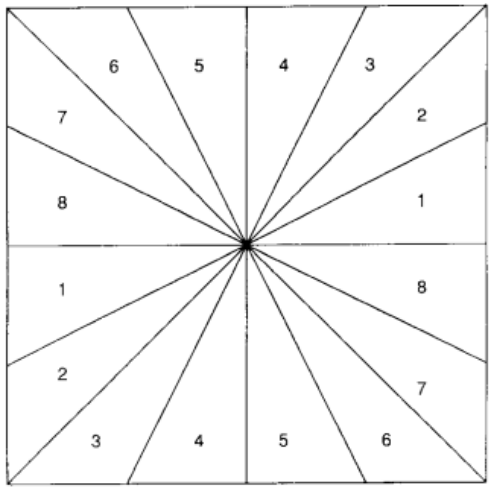

Figure 3.4 Directional Filter Bank [90]

However original partition technique in [19] does not have a high pass property. Authors [31] combined with high direction selectivity with simple high pass (a square placed on middle of frequency domain) filter.

Two versions of Contourlet Transform can be found in the literature. One of them is original Contourlet Transform which uses Laplacian Pyramid technique proposed by [91]. Main idea of this technique is given in Figure 3.5 and can be summarized as follows:

1. First, image is filtered by two filters type (High Pass Filter and Low Pass Filter).
2. Then high passed image fed into the directional filter bank.
3. Directional sub bands are obtained.

4. Low pass filtered image is again filtered by High Pass Filter and Low Pass Filter (Laplacian Pyramid).
5. This process can continue according to user need.

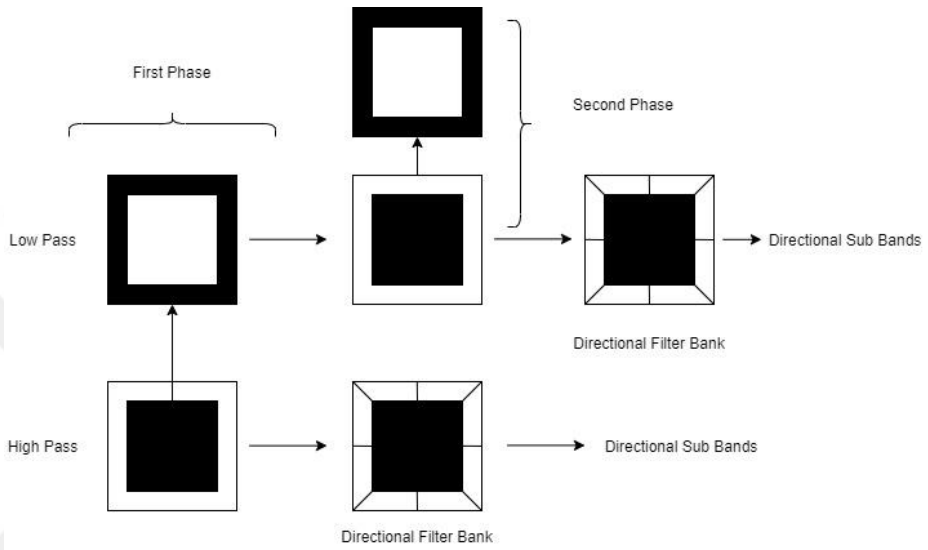

Figure 3.5 Contourlet Transform Schema Using Simple Directional Filter Bank

Another version of the Contourlet Transform is called as Non-Subsampled Contourlet Transform [92]. Although main schema stays the same, authors discard the sampling process (Laplacian Pyramid).

An example of frequency plane division (4) is given in Figure 3.6. Results of these 4 subbands are given in Figure 3.7. High pass is selected as 60.

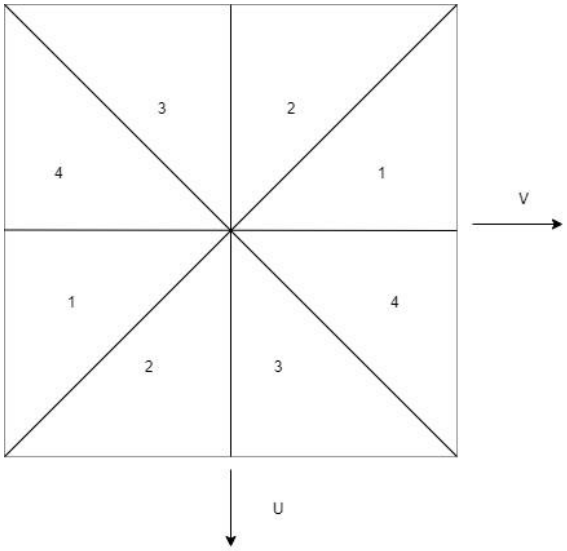

Figure 3.6 Frequency Domain Divided into 4 Directional Subbands

(a)

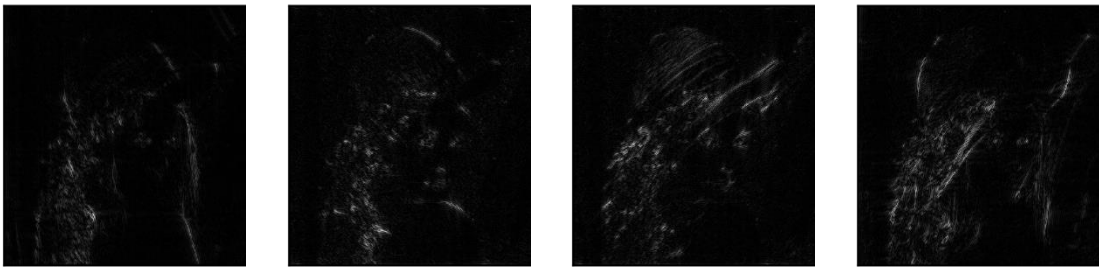

(b) (c) (d) (e)

Figure 3.7 Results of Subbands. (a) 1st Subband, (b) 2nd Subband, (c) 3rd Subband, (d) 4th Subband

As can be seen from Figure 3.7, Contourlet Transform can extract directional features. However, directionality is limited. For example, in Figure 3.7 (a) almost no visuality is achieved. In addition, still some of the features contained in an image are still not visible although more features can be extracted from the frequency domain. To give one more example, frequency plane is divided into eight subbands and its results are given Figure 3.8.

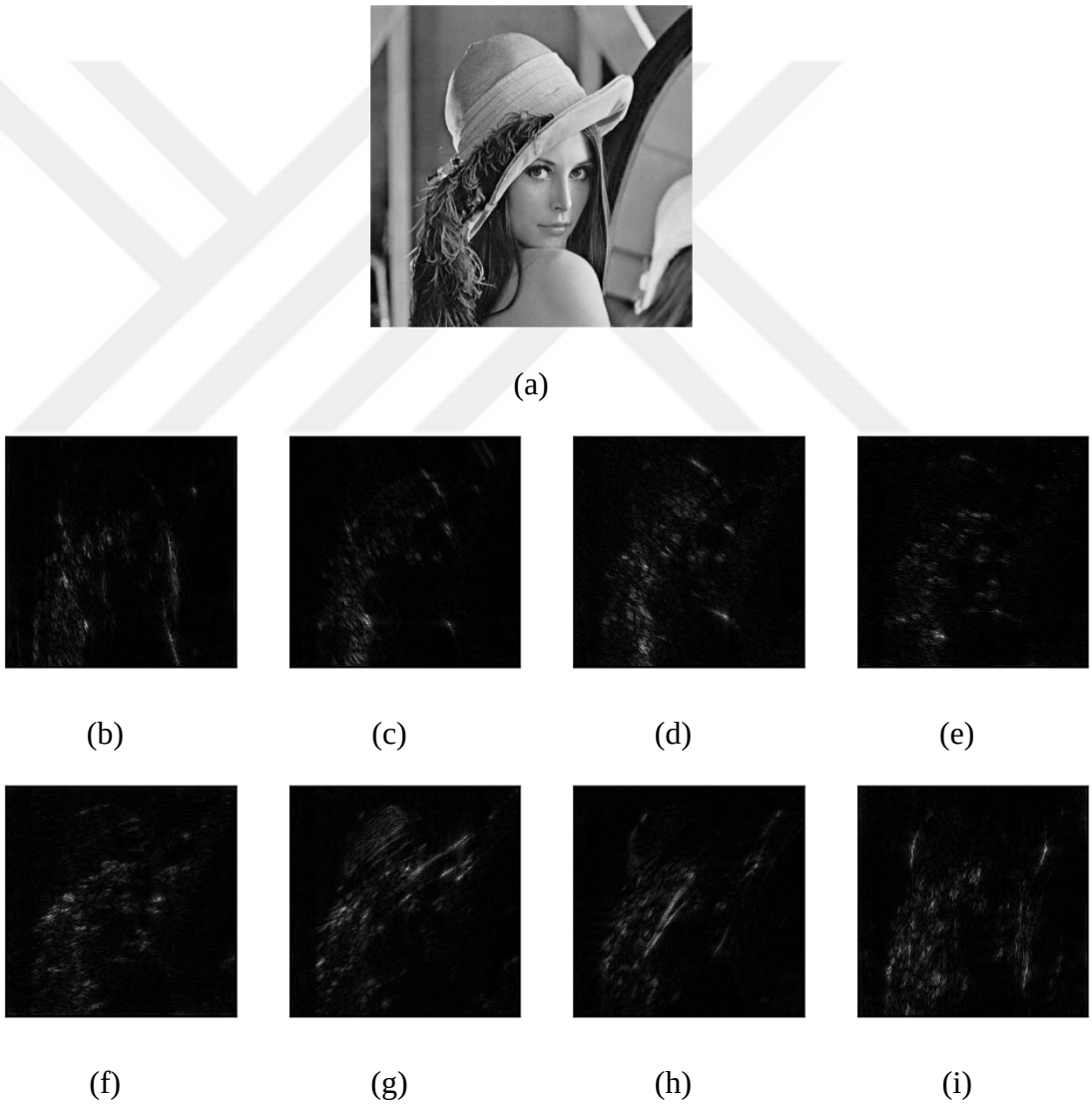

Figure 3.8 Results for Eight Subbands. (b) 1st (c) 2nd (d) 3rd (e) 4th (f) 5th (g)6th (h)7th (i)8th

As can be seen from Figure 3.8 each subband extracts different feature from the original image. However, when using Contourlet Transform schema, features are bounded with

directions meaning that directions cannot be changed freely. Thus, selecting desired angle is not possible. Moreover, as subbands become narrower, feature that is extracted will differ. But when angles are in concern, stability is important, and if the filter shape does not change at every angle, more robust features can be extracted.

In this section, Laplacian Pyramid was not used, only main logic of the Contourlet Transform is considered. Frequency plane can be divided as many directions as user need. Although directions number can be flexible, as number of directions increases coverage area of a direction becomes narrower. Another issue concerning this method, partitions does not fully cover certain part of frequency domain.

3.3 Comments on Steerable Filters

Steerable filters are important in image processing literature since they are able to extract features lies at certain angle which contribute to feature extracting process. Also, it decreases the workload in feature extraction process.

In this section, two of the most used steerable filters in image processing literature is described. One of them 2D Gabor Filter. This filter has been broadly used in the literature. However, 2D Gabor Filter can be regarded weak in some aspects. One weakness of 2D Gabor Filter is that it has a lot of parameters to consider. There are 6 parameters to decide. Each parameter has its own affect in the prepared filter. Another problem regarding 2D Gabor Filter is coverage area in frequency domain. The filter covers only certain parts of the frequency domain, thus lots of filters must be prepared beforehand. Considering these issues, preparing a filter bank in 2D Gabor Filter is a complex and overwhelming process.

Another steerable filter in frequency domain and mentioned in this section is Contourlet Transform. Different from 2D Gabor Filter, Contourlet Transform does not have lots of parameter. The method simply divides frequency plane according to shape of a wedge. Only two parameters can be selected which are direction and a high pass size. However, full control cannot be achieved since the division of frequency plane is constant.

However, more flexible, and more user-friendly filter can be constructed. If the constructed filter can be easily controlled by an angle (not direction as in Contourlet Transform) and a desired high pass type can be changed freely, this could be a great contribution to the literature. For these properties in mind, next section introduces this type of filter. Proposed method uses Lemniscate version of Rose Curve in frequency domain for feature extraction process. Next section deeply analyses proposed method.

CHAPTER 4

PROPOSED METHOD

In previous chapter, two different methods namely 2D Gabor Filter and Contourlet Transform were mentioned.

In 2D Gabor Filter, there are lots of parameters to decide. Each parameter set gives different features of the given image. This brings the problem of parameter selection. Also, there is not a general way of selecting filter parameters. Second important thing about 2D Gabor Filter, in frequency domain Gabor Filter that are specified by a set of parameters extracts only certain frequencies. For other frequencies another filter must be prepared. Although 2D Gabor Filter is a powerful filter type, these two drawbacks of 2D Gabor Filter make it hard to manage.

In Contourlet Transform two issues can be mentioned. First issue is that, since Contourlet Transform divides frequency domain into some number of sub bands, feature extraction process will inevitably be bounded by the number of directions. Another thing about Contourlet Transform is that it needs same certain steps for feature extraction. In each step, image is filtered twice, by one low pass and one high pass filter. High passed image is fed to directional filter banks and features will be extracted and low passed image, which will have been down sampled, again will be high passed and fed into directional filter bank. This process can continue as long as necessary which sometimes can be tiresome.

For these reasons, a new method is proposed for feature extraction. The proposed method works in frequency domain and uses a sinusoid called Rose Curve. The method has advantage of having lesser parameters than mentioned methods and it has the ability to steer, which means features can be extracted using any angle.

4.1 Rose Curve

Rose curves which are also called Rhodonea (Grandi Rose, Multifolium) named after Italian mathematician Guido Grandi. They were named as Rose Curve(s) because these graphs look like roses. Rose Curve(s)'s formula has the following form:

$$A = a\cos(n\theta) \tag{4.1}$$

where, a gives the pedal length of the Rose Curve and n will give number of leaf. Example Rose Curve is given in Figure 4.1. When n is odd Rose Curve has odd leaves, when n is even, Rose Curve has even leaves.

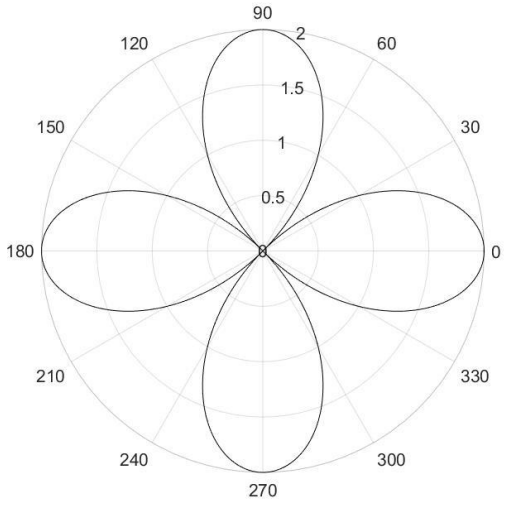

Figure 4.1 An Example Rose Curve. n=4, a=2.

As can be seen in the Figure 4.1, Rose Curve is symmetric with respect to origin. This property of the Rose Curve can be used in frequency domain for feature extraction process. However, although different Rose Curves can be constructed by changing the parameter n, proposed method will focus on only one version of Rose Curve, namely Lemniscate. Next section introduces the Lemniscate version of Rose Curve.

4.2 Lemniscate

One version of Rose Curve is called Lemniscate, which has two leaves symmetric around the origin. A typical Lemnicate formula is given in Equation 4.2 and shape the equation yields is given in Figure 4.2.

$$A^2 = a^2 \cos(2\theta) \quad \textbf{(4.2)}$$

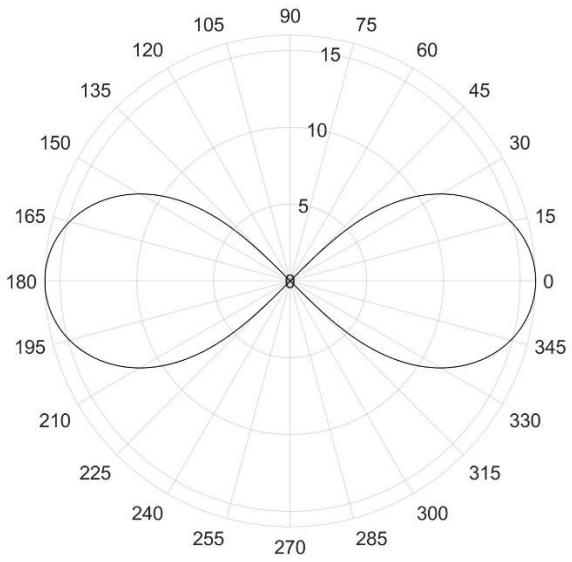

Figure 4.2 An Example of Lemniscate. α=256.

Inspecting the shape more closely can reveal some important property about Lemniscate. Figure 4.2 was drawn in polar coordinates which coordinates are corresponds the angles. And Lemniscate shape could fully cover the horizontal line in Figure 4.2. Also, due to the shape of Lemniscate, its coverage angle can be maximum 45°. As symmetry property is a must in frequency domain for filtering, Lemniscate is a suitable candidate filter type to be used in frequency domain. However, there is one missing parameter for Lemniscate to gain steering property. This property can be achieved by adding a simple parameter. Thus, final, modified formula of Lemniscate is given in Equation 4.3.

$$A^2 = a^2 \cos(2\theta + 2\beta) \quad \textbf{(4.3)}$$

where 2β gives the modified Lemniscate to rotate freely in polar coordinate system. a and 2θ parts stay the same. By placing desired angle into β, we can obtained a Lemniscate rotated in the desired angle (β). Figures obtained by modified Lemniscate formula is given in Figure 4.3.

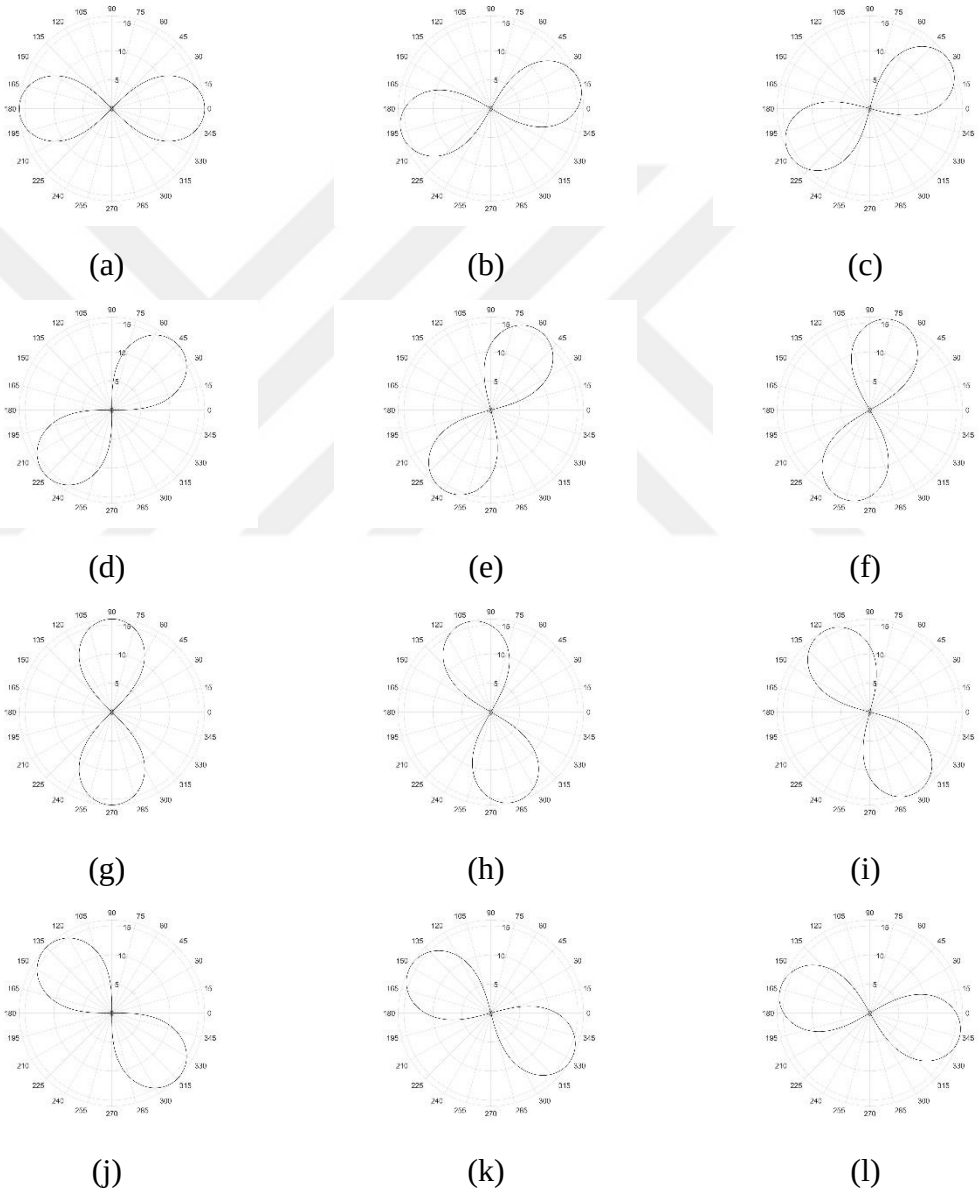

Figure 4.3 Lemniscate Figures with Modified Lemniscate Formula. Angles (β) are between 0˚-165˚ with 15˚ increase respectively. α=256.

If closely inspected, every angle (β) covers the desired angle fully. However, due to shape of the Lemniscate, between -45° and +45° areas also covered partly by Lemniscate. But main points stand, rotation property can be obtained by only one parameter β .

4.3 Lemniscate in Frequency Domain

Drawing Lemniscate in polar coordinates is easy. However, to draw Lemniscate in frequency domain requires slight modification in angle (θ) in the Equation 4.3. In polar coordinate system, θ is given by the user. However, in frequency domain this process must be automatic. Thus, using inverse $\tan$ function θ angle can be obtained. The formula is given in Equation 4.4.

$$\theta = \tan^{-1}\left(\frac{v}{u}\right) \tag{4.4}$$

Where u and v is the frequency domain indexes. By using this technique, desired Lemniscate shape can be drawn in frequency domain. Final formula can be given as in Equation 4.5.

$$A^2 = a^2 \cos\left(2\left(\tan^{-1}\left(\frac{v}{u}\right)\right) + 2\beta\right) \tag{4.5}$$

where a and β are same parameters as given in Equation 4.3. A simple Lemniscate shape drawn in frequency domain is given in Figure 4.4. In Figure 4.4 a pseudo matrix is used as frequency domain.

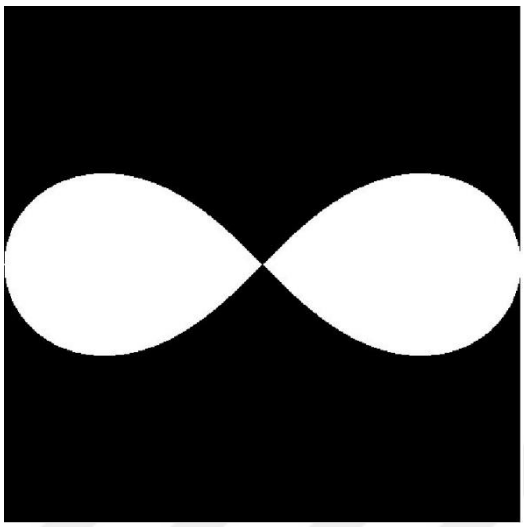

Figure 4.4 An Example Lemniscate in Frequency Domain

Since we have obtained the steering property, this property also can be applied to Lemniscate in frequency domain. 4 different angled Lemniscate figures in frequency domain are given in Figure 4.5. From now on, Lemniscate Filter Type (LFT) abbreviation will be used as proposed method.

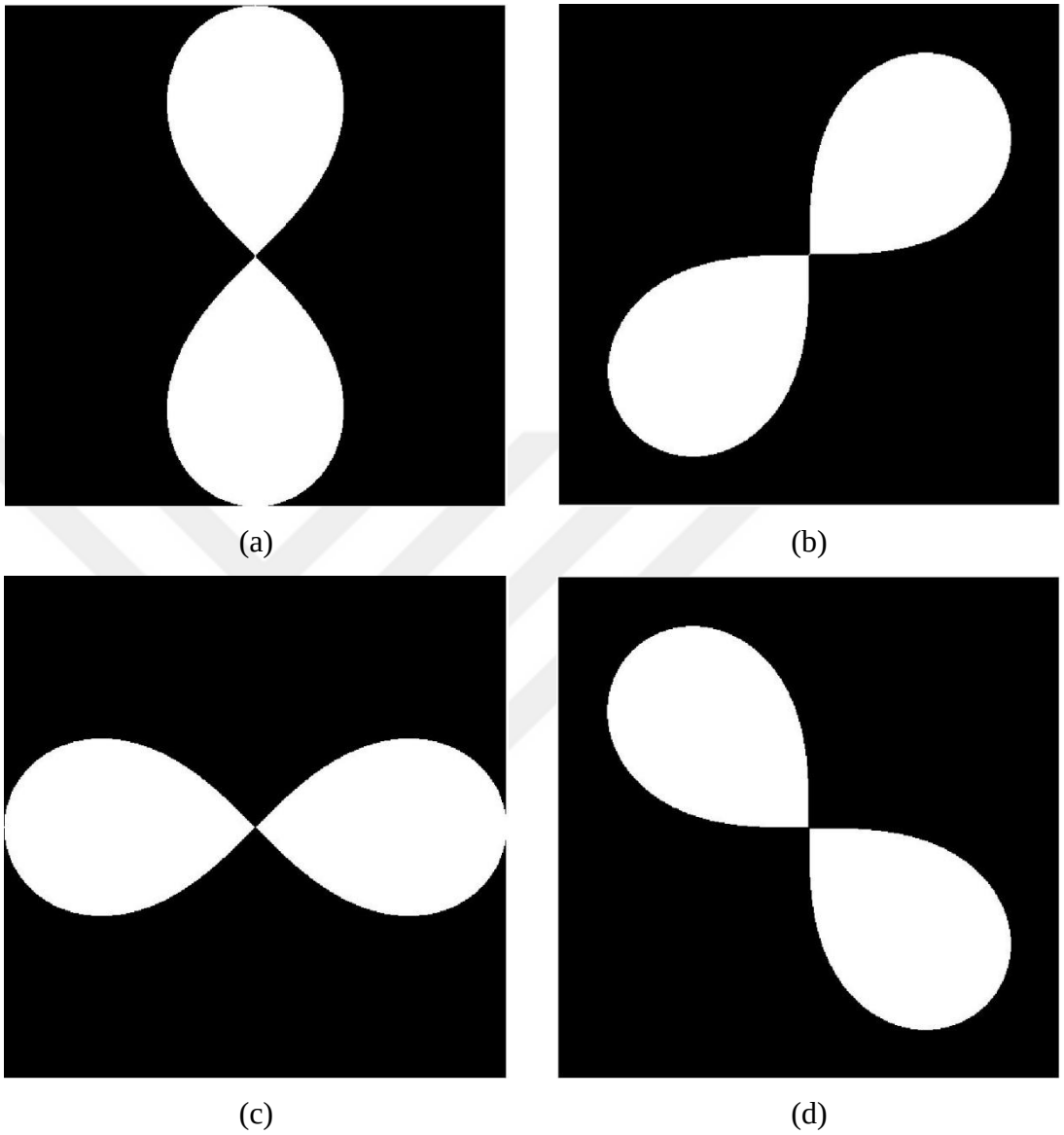

Figure 4.5 Rotated Lemniscates in Frequency Domain. (a)β=0˚, (b)β=45˚, (c)β=90˚, (d)β=135˚

As all desired properties are achieved, Lemniscate can be used as filter in frequency domain. However, using Lemniscate simply in frequency domain as filter yields unwanted results. Since original Lemniscate shape does not suppress frequencies lie at the middle of the frequency domain, resultant image filtered with Lemniscate shape do not contain any meaningful feature. This phenomenon is given in Figure 4.6.

(a)

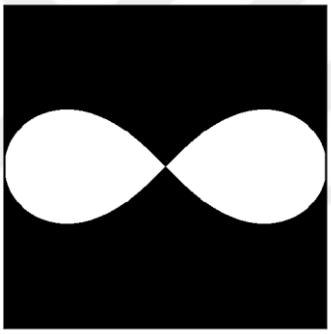

(b) (c)

Figure 4.6 Original Lena Image (512x512). (b) Lemniscate Filter Type in Frequency Domain, (c) Resultant Image Filtered with (b)

As can be seen in Figure 4.6, resultant image (Figure 4.6(c)) does not contain any meaningful feature to be used in later processes. LFT will not produce any usable feature if used like this. Thus, to extract features lie at different angles, LFT must be used with a high pass filter mentioned in Section 2. In the light of such information, main mechanism of LFT can be summarized as follows:

a) Image is filtered with a high pass filter (D_0 is the parameter)

b) Then, the image is filtered with LFT (α - generally half the size of image width or height - and β (between 0°-180°) are the parameters)

c) Finally, a new filter is constructed with three simple parameters. Next 3 sections will describe results, problems, solutions to these problems of LFT when using it with different high pass filter types.

4.4 LFT With Ideal High Pass Filter

LFT can be used with IHPF mentioned in Section 2. Image is firstly filtered with IHPF and strong edges can be extracted in all directions. The image is filtered with LFT further to extract desired angled edges. LFT with IDHPF's result is given in Figure 4.7.

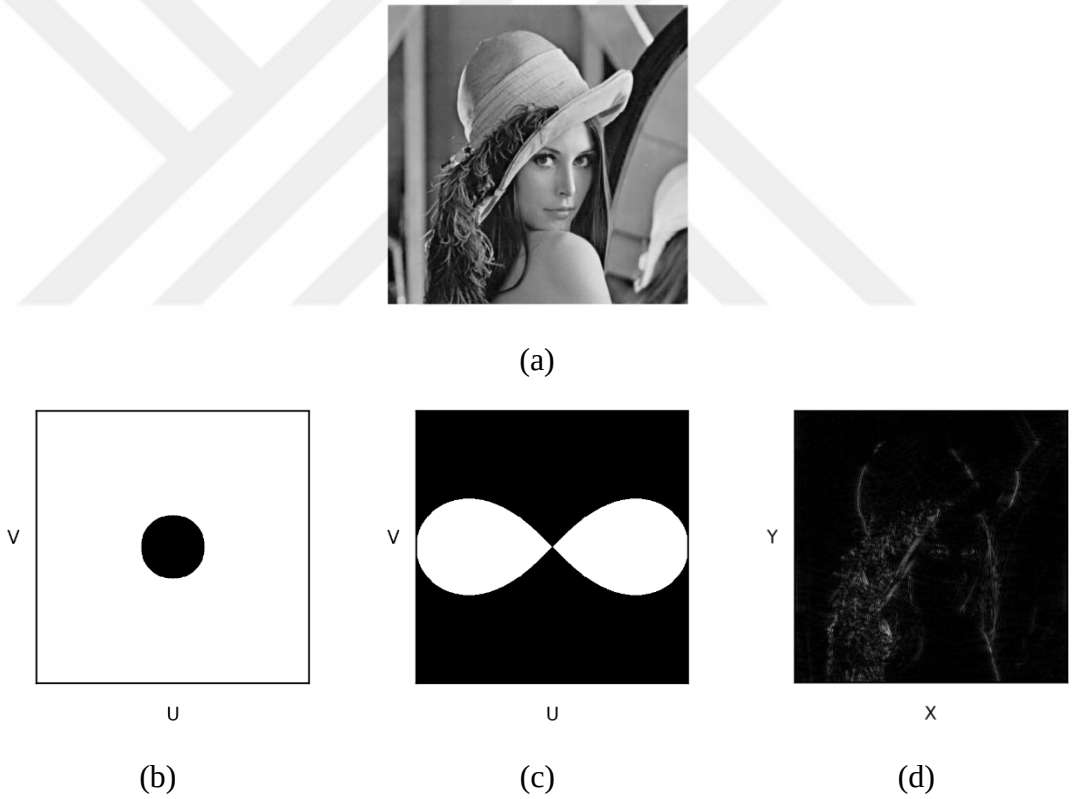

Figure 4.7 An Example of LFT with IHPF. (a) Original Lena Image (512x512), (b) IHPF (D_0=60), (c)LFT (α=256, β=90), (d) Resultant Image.

As can be seen from Figure 4.7 proposed technique can extract features lie at 90° in frequency domain. Also, due to the shape of the Lemniscate, features that are not strictly lie at 90° could be extracted. However, due to the rotation when converting spatial domain to frequency domain, we can extract vertical features of the given image. In fact, features that are intuitively vertical, lie at 90°. Main idea as shown in Figure 4.7, works as intended.

To show the steering property of the LFT, a simple circle is used in experiment shown in Figure 4.8, and as in Figure 4.3, LFT is rotated between 0° and 180° with increase by 15°. And the circle is filtered with each LFT and results are shown in Figure 4.9.

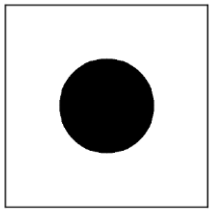

Figure 4.8 A Simple Circle With Radius 120.

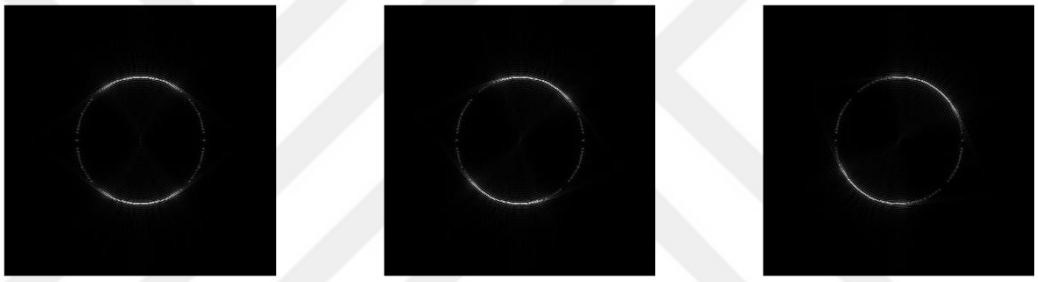

(a) (b) (c)

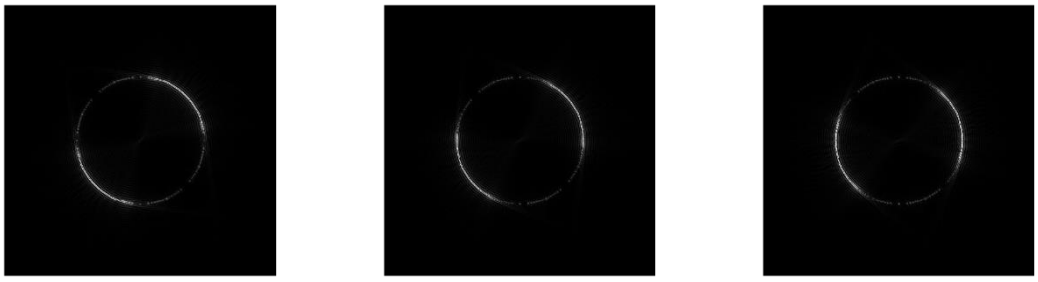

(d) (e) (f)

(g) (h) (i)

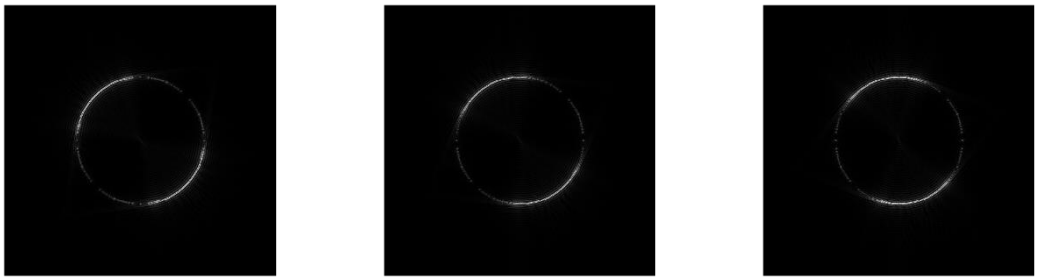

(j) (k) (l)

Figure 4.9 Results of Circle Features Filtered with LFT on 12 Different Angles. βs are between 0° and 180°

As can be seen Figure 4.9, edges lie at all angles in the circle Figure 4.8 were extracted with LFT. However, as mentioned in section 2, IDHPF suffers from ringing effect since transition area in IDHPF is sharp. This effect can be seen from the image Figure 4.7 (d). But to show more clearly, some part of Figure 4.7 (d) is enhanced, and ringing effect is shown in Figure 4.10.

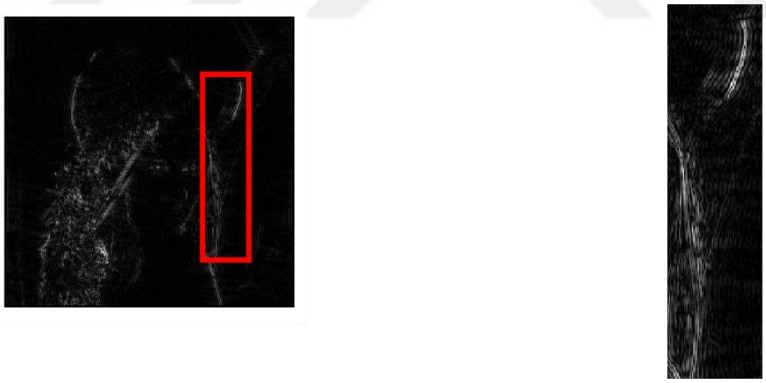

(a) (b)

Figure 4.10 Ringing Effect in IHPF with LFT.

Ringing effect is an effect that is not desired in image processing area. With IHPF, proposed method suffers from ringing effect twice. Because both transitions' (ideal high pass transition and LFT transition) areas are sharp. Some methods have been proposed but, since proposed filter's original idea cannot change, simply changing high pass filter from IDHPF to Gaussian (GHPF) will solve the ringing problem. This solution will only solve the high pass's ringing problem but changing transition areas in LFT also to

Gaussian will solve the ringing problem in general. Next section proposes different version of the proposed method with Gaussian version of both high pass filter and LFT.

4.5 LFT With Gaussian High Pass Filter

LFT can be used with GHPF mentioned in Section 2. The procedure is the same: Image is firstly filtered with GHPF and strong edges can be extracted in all directions. Then image is filtered with LFT. This time transitions are not sharp but has Gaussian shape transition. LFT with GHPF's result is given in Figure 4.11.

(a)

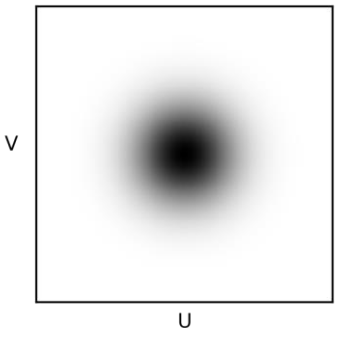

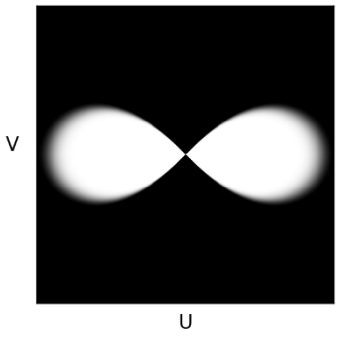

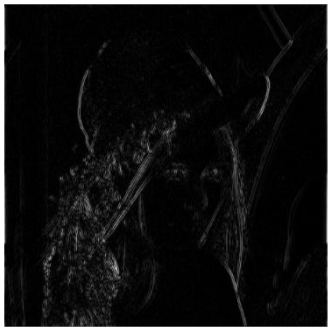

(b) (c) (d)

Figure 4.11 An Example of LFT with GHPF. (a) Original Lena Image (512x512), (b) GHPF (D_0=60), (c)LFT (α=256, β=90, Band Pass Radius=60), (d) Resultant Image.

As can be seen From Figure 4.11 (c), LFT's transition area is now Gaussian and ringing effect problem is now solved greatly by combining LFT with GBPF. Since we use GBPF is used, band pass radius in GPBF must be selected. Since it will increase the parameter

in LFT, we simply choose same value as D_0 in GHPF, which is 60. To show the difference between LFT with IHPF and GHPF, results are shown side by side in Figure 4.12.

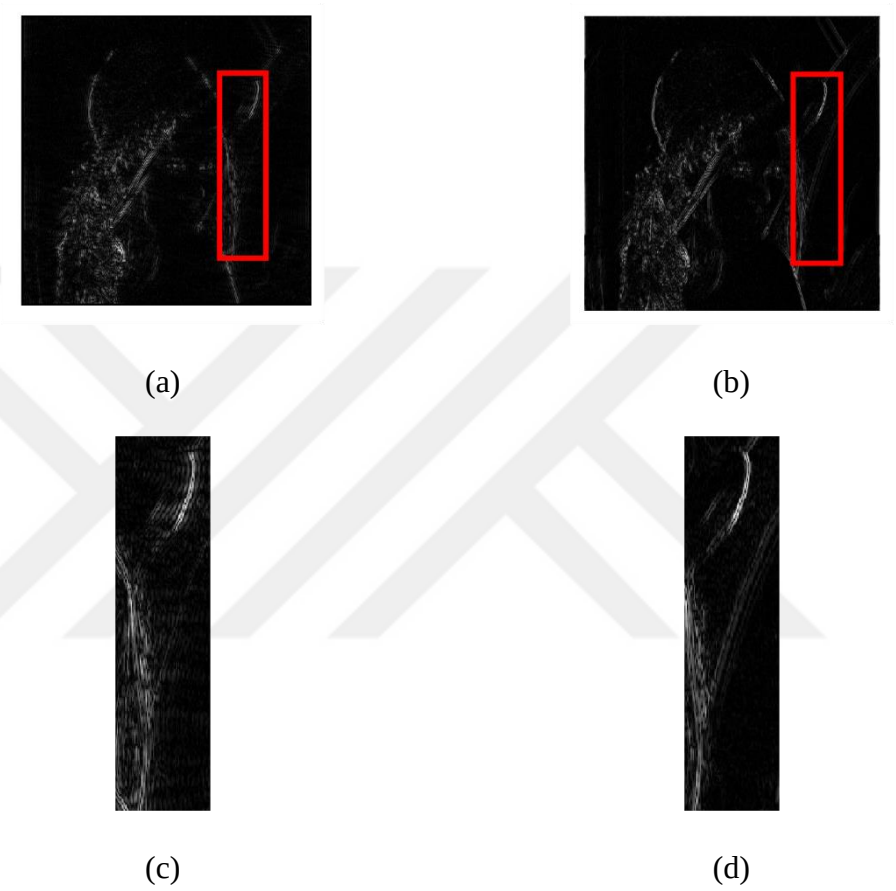

Figure 4.12 Ringing Effect Reduced by LFT combined with GBPF. (a) LFT with IHPF. (b) LFT with GBPF. (c) An Example Enhanced Part of (a). (d) An Example Enhanced Part of (d).

Results shown in Figure 4.12, indicate that when LFT is combined with Gaussian, ringing effect is greatly reduced. Ringing effect is usually done by smoothing the filter by Gaussian filter in the literature, which smooths the whole filter. However, in the proposed method, only edges of the Lemniscate filter are smoothed. Steering property of LFT with GBPF is shown with simple circle (Figure 4.8) is shown in Figure 4.13.

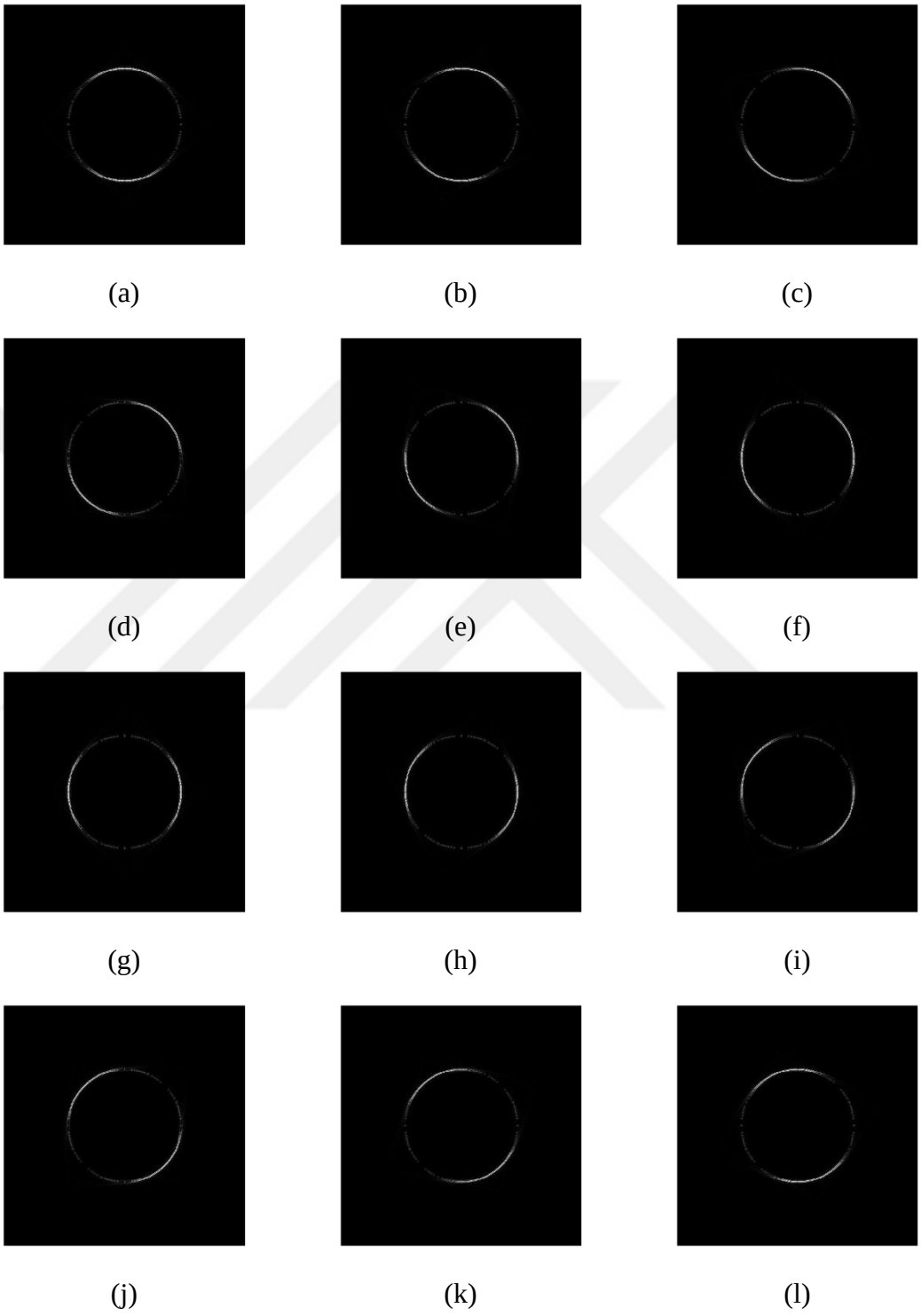

Figure 4.13 Results of Circle Features Filtered with LFT with GBPF on 12 Different Angles. βs are between 0° and 180°.

Also, for all images in Figure 4.13, ringing effect are greatly reduced by GBPF. Finally, another version of LFT can be devised using BHPF and BBPF. Next section introduces third version of LFT.

4.6 LFT With Butterworth High Pass Filter

Final version of LFT is a version combined with both BHPF and BBPF. Similar to previous section, the image first filtered with BHPF then filtered with LFT. Similar to GBPF, BBPF also needs a parameter D_0. To not to increase the number of parameters, BBPF's D_0 is selected as same as BHPF's D_0. However, in Butterworth Filter, there is a parameter cannot be avoided, the parameter n that controls the order of the filter. When using the LFT with Butterworth, this extra parameter must be considered. This parameter, as other parameters, is at user pleasure. Result of LFT with BHPF and BBPF is given in Figure 4.14.

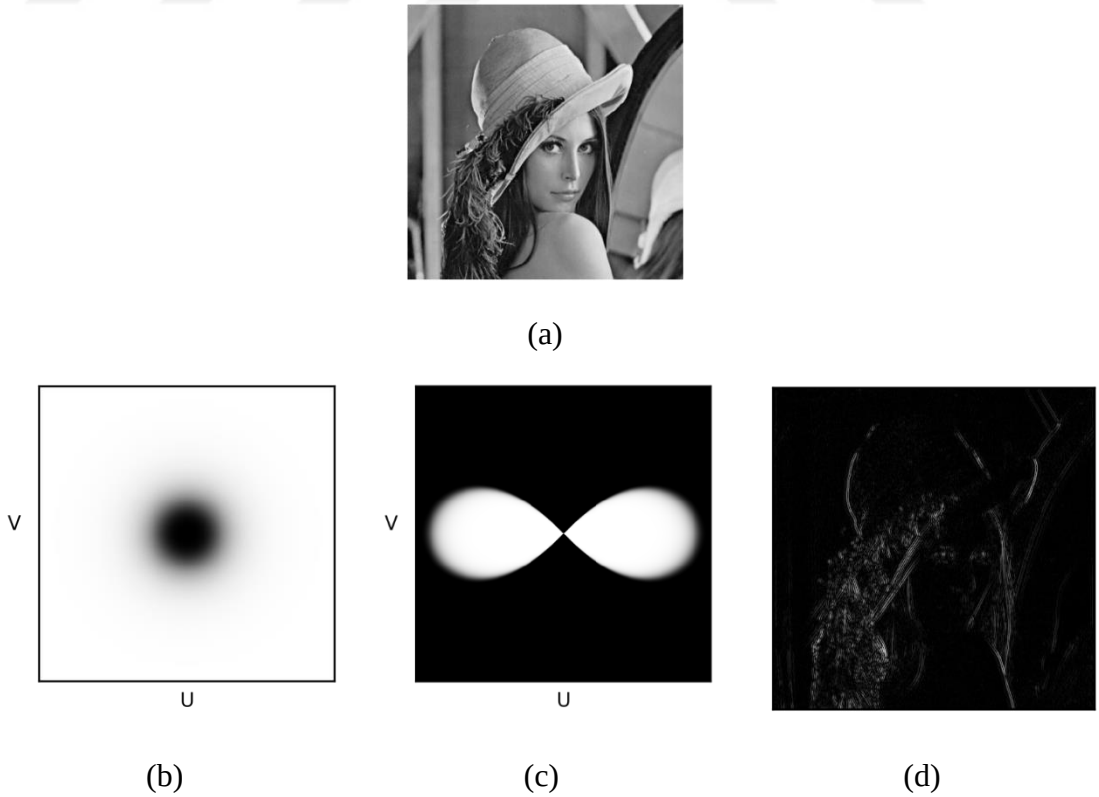

Figure 4.14 An Example of LFT with IHPF. (a) Original Lena Image (512x512), (b) BHPF (D_0=60), (c)LFT (α=256, β=90, n=2, Band Pass Radius = 60), (d) Resultant Image.

As in section 4.4 and 4.5, circle is filtered with BHPF then LFT with BBPF and its results are given in Figure 4.15.

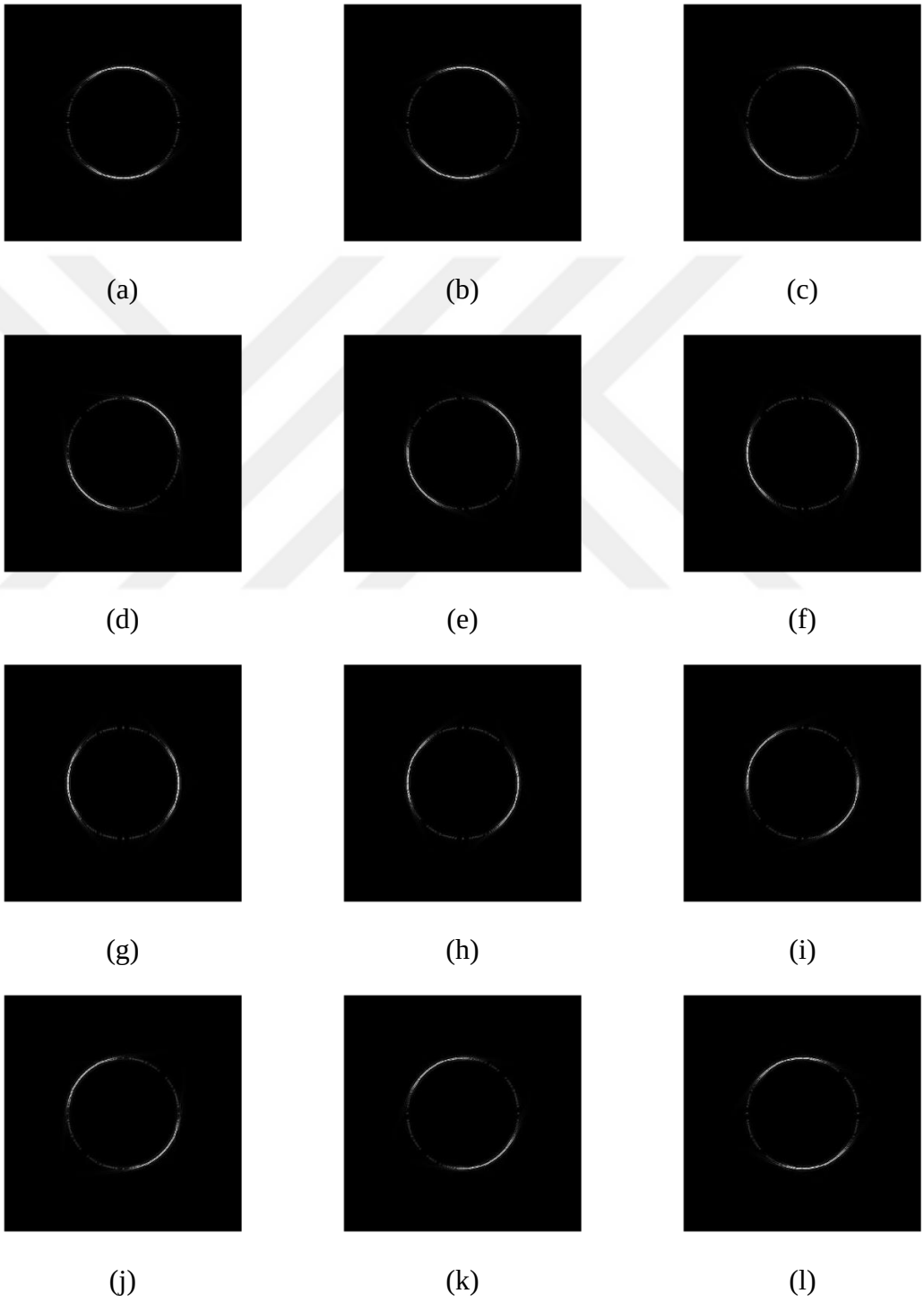

Figure 4.15 Results of Circle Features Filtered with LFT with BBPF on 12 Different Angles. βs are between 0° and 180°.

4.7 Comments on LFT

In this section, a fully steerable filter performs in frequency domain is proposed. Furthermore, three different types of the proposed filter type are introduced. Also, this filter type is superior to filters mentioned in Section 3 in some respects.

Firstly, proposed filter has less parameters than 2D Gabor Filters. The proposed filter type has only 3 parameters. One parameter, a high pass radius (D_0) selected by the user according the type of high pass filter (Ideal High Pass, Gaussian High Pass, Butterworth High Pass). Second parameter is the angle parameter (β) to control the angle. This β parameter is the original contribution to Lemniscate formula which enables it to rotate freely. The parameter β should be between 0° - 180°. Since proposed filter type symmetric around the origin, mentioned angles are sufficient to extract features lie at any angle in frequency domain.

Secondly, the proposed filter overcomes the angle problem in Contourlet Transform. Contourlet Transform does not have the full control over the frequency domain. Thus, frequency domain is divided into constant wedges. However, with the proposed filter user can easily manipulate the β parameter for angles in frequency domain.

Although main idea of the proposed filter is angle property, one other important property is length of the Lemniscate (α). In all examples, α was kept constant which is half size of the image. In proposed filter type mentioned parameter can be used like in the examples given in this thesis.

However, by manipulating other parameter, D_0, different features lie at any angle can be extracted. By keeping α parameter half size of the given image, one can change D_0 as needed. For example, if D_0 becomes bigger each time, higher frequencies at desired angle can be extracted. Next section will give full examples about this procedure.

Until now, the proposed method only sample images. However, to show the capability on the datasets that publicly available and has been studied in the literature is still needed.

Next section will be about the Facial Expression Recognition (FER) classification using proposed method.

CHAPTER 5
EXPERIMENTAL RESULTS AND DISCUSSION

Previous chapter, the proposed method was evaluated visually. To evaluate the performance of the LFT, the proposed filter was used in a classification problem. For the classification problem, facial expression classification is selected. This problem has been studied on the literature widely and different approaches have been proposed. Simply, a facial expression is the feeling which emerges on a human face. A facial expression can be divided into seven different categories [93].

These expressions are:

- Anger
- Disgust
- Fear
- Happiness
- Sadness
- Surprise
- Neutrality

Classification of these expressions by image processing techniques is an active research area and generally can be divided into two categories.

First category which is outside of the scope of this thesis is classification of facial expressions with CNNs [94,95]. However, CNNs extract feature without user intervention and suffers from high number of parameters. Second category is classification of facial expressions by using hand-crafted features extracted from the faces, then feeding these hand-crafted features into any classification algorithm [96-98]. However, when using this

technique, deciding of a feature that represent the expression good enough is a problem, furthermore, deciding parameters for hand crafted feature extraction method is another problem.

However, simplicity of the proposed method can be used in this classification problem. it was hypothesized that FER classification can be simplified by LFT. Dataset for FER classification was selected CK+48 since it is publicly available.

5.1 Dataset (CK+48)

The CK+48 dataset contains 7 different facial emotions. There are two versions of this set, CK and CK+48. However, CK+48 is a more descriptive dataset. An example for each emotion is given in Figure 5.1. Also, the number of images in each category is given in Table 5.1.

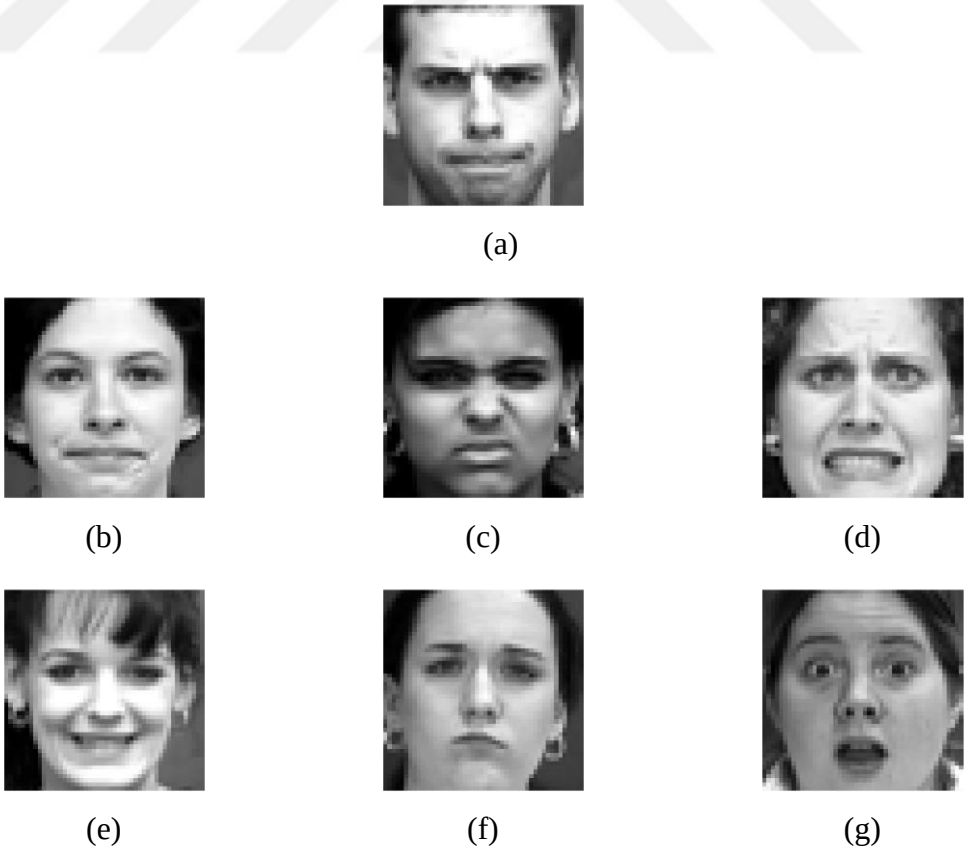

Figure 5.1 Examples of Facial Expressions. (a) Anger, (b) Contempt, (c) Disgust, (d) Fear, (e) Happy, (f) Sadness, (g) Surprise

Table 5.1 Number of Images in Each Category

Category	Number of Images
Anger	135
Contempt	54
Disgust	177
Fear	75
Happy	207
Sadness	84
Surprise	249

Table 5.1 shows the number of images in each category. Since each category contains different number of images, 54 images in each category randomly selected for the experiments to forestall the bias.

As can be seen in Figure 5.1 each expression has particular pattern. Furthermore, if the images are closely examined, it can be easily seen that main features of an expression surface in a face can be divided into two parts, namely eyes and lips. To show this hypothesize, each face in Figure 5.1 is divided into two parts which are given in Figure 5.2.

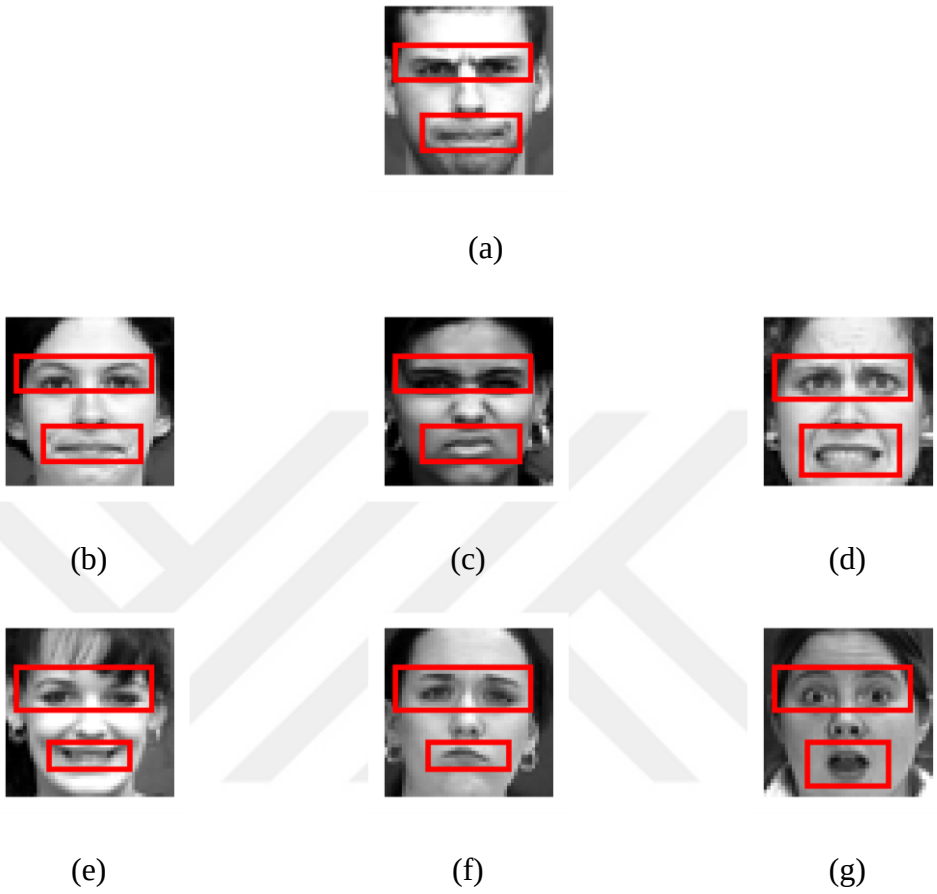

Figure 5.2 The Most Distinguishable Parts in Facial Expressions. (a) Anger, (b) Contempt, (c) Disgust, (d) Fear, (e) Happy, (f) Sadness, (g) Surprise

Also, again, if closely examined, all mentioned features in Figure 5.2. appear in certain angle, namely horizontal (90°) (Upward direction according to coordinate system considered as 0°). As the proposed filter has flexibility in angle selection, the boxed regions can be easily extracted in frequency domain. The forthcoming section explains the method in feature extraction.

5.2 Feature Extraction Method

As mentioned, features that make major contribution in facial expression is generally eyes and the lips. In other saying, extracting features from these parts can successfully represent the main expression arise in the face. These mentioned features could be extracted by the filter given in Figure 5.3.

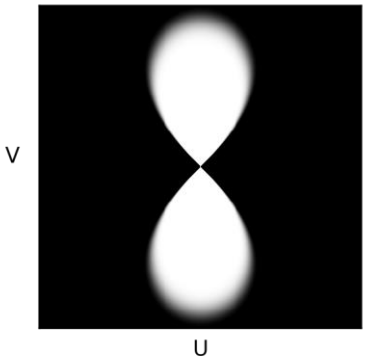

Figure 5.3 Proposed Filter Rotation in Frequency Domain to Extract Features

Before beginning the feature extraction process, all images in the dataset are resized into 64x64. For the LFT parameters, length of one side of the leaf (α) was selected as 32. To reduce the ringing effect problem, LFT was used with GBPF. As a high pass radius, LFT was used with three different high pass radius sizes (35,45,55).

Reason of using high pass filters with different radiuses was to extract more distinctive features from the images which main reason of this procedure will be given shortly. In general, for feature extraction process, there are only three filters that are shown in Figure 5.4.

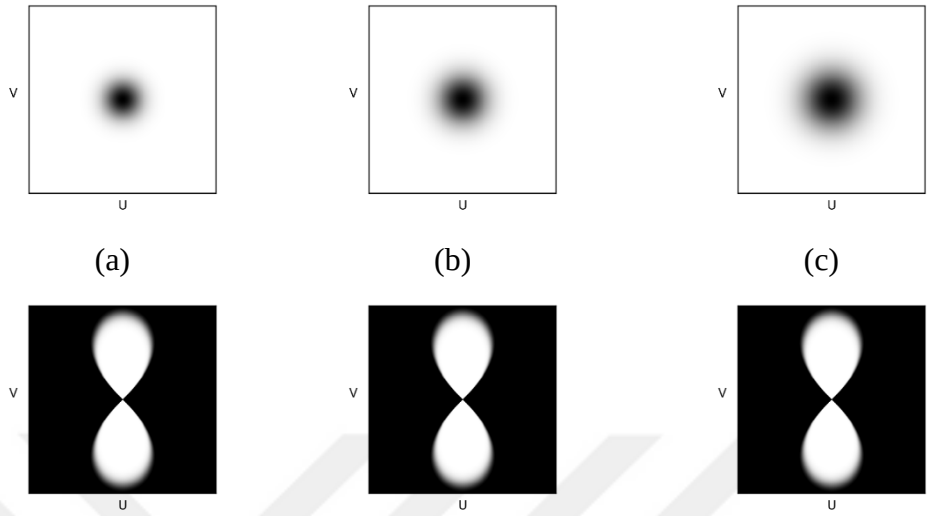

Figure 5.4 Prepared Filters. (a) GHPF (D_0=35), (b) GHPF (D_0=45), (c) GHPF (D_0=55) (d,e,f) LFT with α=32.

First, the images in the dataset were filtered with GHPF shown in Figure 5.4 (a), further, the images were filtered with LFT also shown in Figure 5.4 (b). Same procedure was applied again for Figure 5.4 (b)-(d). These filter types were named as Type-I, Type-II, Type-III respectively. An example of features extracted from each expression is given in Figure 5.5.

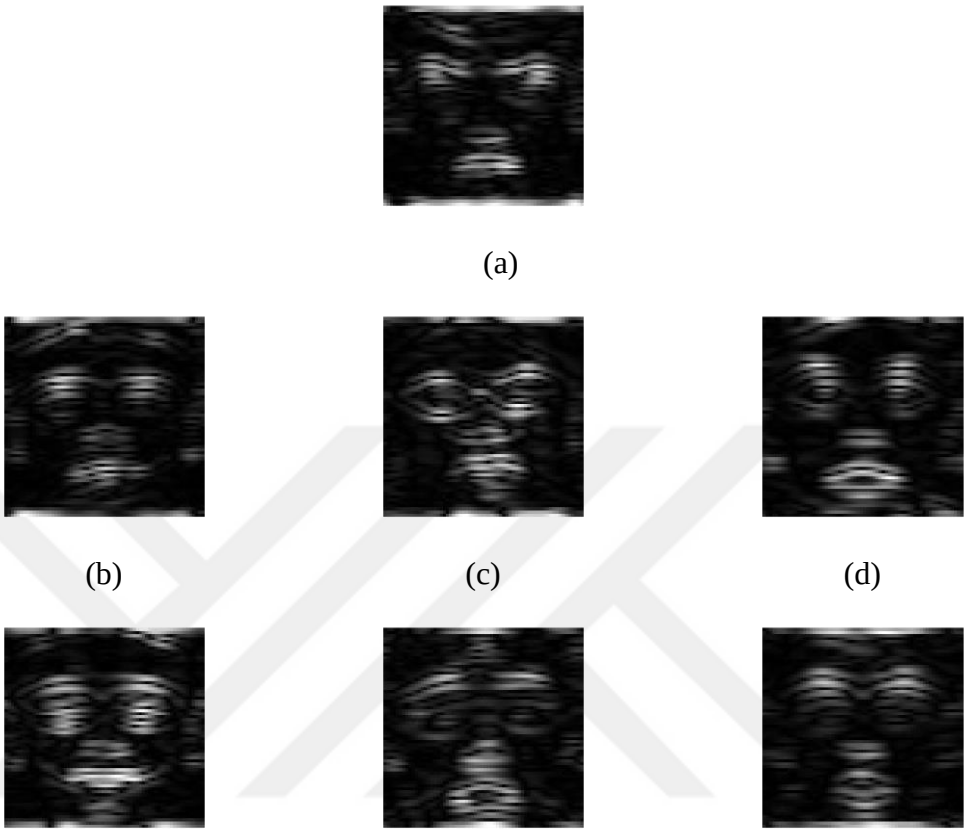

(a) (b) (c) (d) (e) (f) (g)

Figure 5.5 Features Extracted with the Proposed Method. (a) Anger, (b) Contempt, (c) Disgust, (d) Fear, (e) Happy, (f) Sadness, (g) Surprise.

Main reason of using three different high pass filter with different high pass radiuses was to extract more robust features, since as the radius gets bigger, higher frequencies (sharper edges in spatial domain) can be extracted. This hypothesis can be seen in Figure 5.6.

(a) (b) (c)

Figure 5.6 Effect of High Pass Radius. Emotion is Anger. (a) D_0=35, (b) D_0=45, (c) D_0=55.

Horizontal features of the images in the dataset successfully were extracted. Since the proposed filter has curved shape of the proposed filter, these curved features (especially eyebrows) can be extracted. One can successfully differentiate one expression from another. However, to automatically detect these expressions, the features must be fed into a machine learning algorithm and quantitatively analyzed. Before feeding these features into machine learning algorithms, the images are flattened, normalized, and fed into the algorithms. Since the images are 64x64, filtered images are also 64x64, thus flattened feature vector has a size of 4096.

5.3 Experimental Results

Selected machine learning algorithm was Support Vector Machine (SVM) [99] with linear kernel. SVM is a supervised machine learning algorithm means that labelled data are fed into algorithm beforehand. It is used in diverse applications such as intrusion detection, medical classification, spam-mail classification etc. The algorithm basically divides points of data with the largest possible amount of margin. A simple SVM figure is given in Figure 5.7.

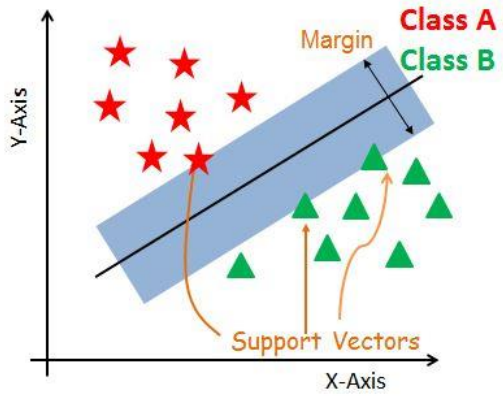

Figure 5.7 - A Simple SVM Working Logic [100]

The experiment was also validated by using Stratified K-Fold Cross Validation. The overall set was divided into 10-folds, and at each run 1-fold was removed for testing and

other 9 were used in training. Stratified K-Fold Cross Validation schema is given in Figure 5.8.

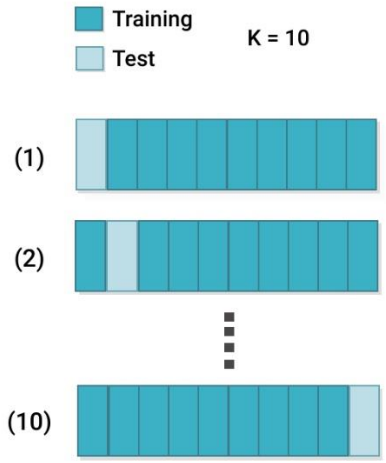

Figure 5.8 - A Simple 10-Folds Cross Validation [101]

Average accuracy (Eq. 5.1) result of 10-folds cross validation was presented as a result. Average precision (Eq. 5.2), average recall (Eq. 5.3), and average F1 Score (Eq. 5.4) were calculated for the algorithm.

$$Accuracy = \frac{TP + TN}{TP + TN + FP + FN} \quad \textbf{(5.1)}$$

$$Precision = \frac{TP}{TP + FP} \quad \textbf{(5.2)}$$

$$Recall = \frac{TP}{TP + FN} \quad \textbf{(5.3)}$$

$$F - Measure = \frac{2 \times precision \times recall}{precision + recall} \quad \textbf{(5.4)}$$

TP, TN, FP and FN denote the number of true positives, false positives, true negatives, and false negatives respectively. For all experiments Python language and Python's sklearn library were used. Results for the SVM algorithm is given in Table 5.2.

Table 5.2 Results for the Proposed Method

Filter(s) Used	Results	
Type I	**Average Accuracy**	%71.42
	Average Precision	%70.47
	Average Recall	%71.42
	Average F Measure	%68.47
Type I & Type II	**Average Accuracy**	%97.85
	Average Precision	%97.38
	Average Recall	%97.33
	Average F Measure	%97.85
Type I & Type II & Type III	**Average Accuracy**	%97.14
	Average Precision	%98.09
	Average Recall	%97.14
	Average F Measure	%96.95

As can be seen from the Table 5.2, the proposed method achieved good performance for all metrics. For the Type I, results suggest that SVM algorithm did not separate the emotion classes successfully. This can be because of the lack of enough data for the algorithm to perform successfully. All four metrics for Type I resulted around %70 which was not enough for a successful classification. However, for the Type II, we can see that an acceptable accuracy for the experiment was achieved. This means that the SVM algorithm had enough data to discriminate the classes successfully. All metrics for Type I & Type II resulted around %97 which was enough for a successful classification.

For the final type (Type I & Type II & Type III), results suggest that proposed mechanism reached its highest accuracy. If examined closely, the result of last two combinations of the Types do not differ significantly. Moreover, it can be stated that second version (Type I& Type II) of the proposed mechanism achieved better results than third version (Type I & Type II & Type III). This indicates that only two filters are sufficient for the SVM to correctly classify the facial expressions.

Due to the stochastic nature of the SVM algorithm, its exact behavior cannot be foreseen, however experiments showed that all metrics has not been gone under %95 when more than one type was combined.

The proposed method's result was also compared some of the recent works in the literature. As mentioned before proposed method uses hand crafted features, which is different from CNN logic. Thus, studies that were compared only use hand crafted features. Study that was published in 2019 [102] achieved accuracy of %94.42. Similar to this thesis, results were presented as average of 10-fold cross validation. However, authors did not mention about precision, recall and F1 metrics in their works. Also, authors applied different preprocessing techniques on the images for their experiments. However, results indicate that the proposed feature extraction method with the proposed filter surpassed the mentioned study.

Another study [103] which did experiment in the same dataset combined 2D Gabor Filter and Local Binary Pattern (LBP) and achieved %95.45 with SVM linear kernel. The proposed method also surpassed the mentioned study. Comparisons of the mentioned studies with the current one is given in Table 5.3.

Table 5.3 Comparison of Studies in Terms of Recognition Rates

Methods	**Recognition Rate**
[102]	%94.42
[103]	%95.45
Current Method (Type I-II-III)	%97.14

Main distinction between proposed method and methods mentioned in those papers [102-103] can be divided into two. First distinction is that the filter which was proposed. The proposed filter showed that, feature from any angle in frequency domain can be successfully, and more important, extracted easily. To the best of our knowledge, this flexibility is a new property when frequency domain is in concern.

Another distinction is using only three filters, acceptable percentages for all metrics were achieved. This shows that, proposed filter can extract meaningful features and can be used for further processes.

CHAPTER 6
CONCLUSION

Feature extraction in image processing is the most important part for any application in computer vision. Thus, feature extractions methods that are both simple and flexible are also important. These methods can be divided into two. One of them is feature extraction in spatial domain, another one in feature extraction in frequency domain. In spatial domain, extraction of a feature lies in certain direction is hard and complex process. However, in frequency domain, directional features extraction is easier. Proposed methods for feature extraction in frequency domain either are generally have myriad number of parameters or does not have flexible in angle selection.

In this thesis, a novel feature extraction method in frequency domain is proposed. The method has been inspired by certain shape called Lemniscate, a version of Rose Curve. Process of feature extraction with Lemniscate is twofold. First, image in frequency domain is filtered with desired high pass type (Ideal, Gaussian or Butterworth), then the image is filtered with Lemniscate shape with desired angle. Thus, proposed filter has only two parameters. The length of the Lemniscate is remained constant in this thesis and selected as half of the given image. However, if length of the lemniscate is considered as a parameter, the proposed method will have only three fully customizable parameters.

The proposed filter was tested on a Facial Expression classification problem using publicly available dataset CK+48. For algorithms, three different machine learning algorithms was selected. Results obtained from the experiment suggested that the proposed filter is achieved reasonable results. Also, results were compared to some of the recent studies, results also suggested that results in this thesis surpassed the studies mentioned.

For future studies, following contributions can be made for further improvements:

- Since the proposed filter has small number of parameters, it can be combined with a genetic algorithm for optimization of the parameters. Thus, selection of parameters can be decided automatically.
- Although, features that are extracted from the images can be fed into machine learning algorithms, this feature extraction process also can be regarded as pre-processing. Thus, images that are filtered with the proposed method can be fed into a CNN network to increase the performance of the CNN structure.

REFERENCES

[1] Kumar, G., & Bhatia, P. K., "A detailed review of feature extraction in image processing systems" *In 4th International conference on advanced computing & communication technologies*, pp. 5-12. 2014.

[2] Ping Tian, D., "A review on image feature extraction and representation techniques", *International Journal of Multimedia and Ubiquitous Engineering*, Vol.8, pp. 385-396, 2013.

[3] Bai, Y., Guo, L., Jin, L., & Huang, Q., "A novel feature extraction method using pyramid histogram of orientation gradients for smile recognition" *In 16th IEEE International Conference on Image Processing*, pp. 3305-3308, 2009.

[4] Mohanaiah, P., Sathyanarayana, P., & GuruKumar, L. "Image texture feature extraction using GLCM approach", *International Journal of Scientific and Research Publications*, Vol. 3, pp. 1-5, 2013.

[5] Gonzalez, R. C., & Woods, R. E., *Digital Image Processing*. USA. Prentice-Hall. 2002.

[6] Gao, W., Zhang, X., Yang, L., & Liu, H. "An improved Sobel edge detection", *In 3rd International Conference on Computer Science and Information Technology*, pp. 67-71, 2010.

[7] El-Khamy, S. E., Lotfy, M., & El-Yamany, N. "A modified fuzzy Sobel edge detector", *In Proceedings of the Seventeenth National Radio Science Conference*. pp. C32-1. 2000.

[8] Ying-Dong, Q., Cheng-Song, C., San-Ben, C., & Jin-Quan, L. "A fast subpixel edge detection method using Sobel–Zernike moments operator", *Image and Vision Computing*, Vol 23, pp. 11-17. 2005.

[9] Fukushima, K., & Miyake, S., "Neocognitron: A self-organizing neural network model for a mechanism of visual pattern recognition", *In Competition and cooperation in neural nets*. pp. 267-285. 1982.

[10] LeCun, Y., Haffner, P., Bottou, L., & Bengio, Y., "Object recognition with gradient-based learning", *In Shape, Contour and Grouping in Computer Vision*. pp. 319-345. 1999.

[11] Liu, W., Wang, Z., Liu, X., Zeng, N., Liu, Y., & Alsaadi, F. E., "A survey of deep neural network architectures and their applications", *Neurocomputing*, Vol. 234, pp.11-26. 2017.

[12] Liu, M., Jiao, L., Liu, X., Li, L., Liu, F., & Yang, S., "C-CNN: Contourlet Convolutional Neural Networks", *IEEE Transactions on Neural Networks and Learning Systems*. Vol. 32, pp. 2636-2649. 2020.

[13] Jourabloo, A., Ye, M., Liu, X., & Ren, L., "Pose-invariant face alignment with a single cnn", *In Proceedings of the IEEE International Conference on Computer Vision*. pp. 3200-3209. 2017.

[14] More, S., Shirodkar, V., Joshi, R., & Thakur, N. "Overcoming the Drawbacks of Convolutional Neural Network Using Capsule Network", *IOSR Journal of Computer Engineering*, Vol 21. pp. 06-11. 2019.

[15] Chakrabarti, S, & Mitra, S. K., "Design of two-dimensional digital filters via spectral transformations", *Proceedings of the IEEE*, Vol. 65, pp. 905-914. 1977.

[16] Harn, L, & Shenoi, B., "Design of stable two-dimensional IIR filters using digital spectral transformations". *IEEE Transactions on Circuits and Systems*, Vol. 33. 483-490. 1986.

[17] Tosic, D. V, et al., "Symbolic approach to 2D biorthogonal diamond-shaped filter design", *21st Int. Conf. on Microelectronics*, Vol. 2, pp. 709-712, 1997.

[18] Simoncelli, E. P, & Farid, H. “Steerable wedge filters for local orientation analysis”, *IEEE Transactions on Image Processing*, Vol. 5, pp. 1377-1382, 1996.

[19] Bamberger, R, & Smith, M. (1992). “A filter bank for the directional decomposition of images: theory and design”, *IEEE Trans. Signal Processing*, Vol. 40, 882-893, 1992.

[20] Qunshan Gu and M. N. S. Swamy, “On the design of a broad class of 2-D recursive digital filters with fan, diamond and elliptically-symmetric responses,” *In IEEE Transactions on Circuits and Systems II: Analog and Digital Signal Processing*, Vol. 41, No. 9, pp. 603-614, 1994.

[21] Zhou, Z. F., Cheng, Y. Y., & Shui, P. L., “Construction of 2-D directional filter bank by cascading checkerboard-shaped filter pair and CMFB”. *Signal processing*, Vol. 88, No. 10, pp. 2500-2510, 2008.

[22] Truc, P. T., Khan, M. A., Lee, Y. K., Lee, S., & Kim, T. S., “Vessel enhancement filter using directional filter bank”. *Computer Vision and Image Understanding*, Vol.113, No 1, pp. 101-112, 2009.

[23] Vandergheynst, P., & Gobbers, J. F., “Directional dyadic wavelet transforms: Design and algorithms”. *IEEE transactions on image processing*, Vol. 11, No. 4, pp. 363-372, 2002.

[24] Nguyen, T. T., & Oraintara, S. (2004, May). “A directional decomposition: Theory, design, and implementation”. *In 2004 IEEE International Symposium on Circuits and Systems*, Vol. 3, pp. 281-284, 2004.

[25] Park, S. I., Smith, M. J., & Mersereau, R. M., “Improved structures of maximally decimated directional filter banks for spatial image analysis”, *IEEE Transactions on Image Processing*, Vol. 13, No. 11, pp. 1424-1431, 2004.

[26] Eslami, R., & Radha, H., "A new family of nonredundant transforms using hybrid wavelets and directional filter banks", *IEEE Transactions on image processing*, Vol. 16, No. 4, pp. 1152-1167, 2007.

[27] Shi, G., Liang, L., & Xie, X., "Design of directional filter banks with arbitrary number of subbands", *IEEE transactions on signal processing*, Vol. 57, No.12, pp. 4936-4941, 2009.

[28] Lu, Y. M., & Do, M. N., "Multidimensional directional filter banks and surfacelets", *IEEE Transactions on Image Processing*, Vol. 16, No. 4, pp. 918-931, 2007.

[29] Park, C. H., Lee, J. J., Smith, M. J., Park, S. I., & Park, K. H., "Directional filter bank-based fingerprint feature extraction and matching", *IEEE Transactions on Circuits and Systems for Video Technology*, Vol.14, No.1, pp. 74-85, 2004.

[30] Yong Ching Lim and Seo How Low, "The synthesis of sharp diamond-shaped filters using the frequency response masking approach," *IEEE International Conference on Acoustics, Speech, and Signal Processing*, Vol 3, pp. 2181-2184, 1997.

[31] Do MN, Vetterli M., "Contourlets: A directional multiresolution image representation", *In Proceedings of the IEEE International Conference on Image Processing*, Vol. 1, pp. 357-360, 2002.

[32] Meyer, Y., "Wavelets and Operators", Cambridge university press. Vol. 1, No. 37, 1992.

[33] Moayedi, F., Azimifar, Z., Boostani, R., & Katebi, S., "Contourlet-based mammography mass classification using the SVM family". *Computers in Biology and Medicine*, Vol. 40, No. 4, pp. 373-383, 2010.

[34] Liu, Y., Zhang, C., Cheng, J., Chen, X., & Wang, Z. J., "A multi-scale data fusion framework for bone age assessment with convolutional neural networks", *Computers in Biology and Medicine*, Vol. 108, pp. 161-173, 2019.

[35] Patil, H. Y., Kothari, A. G., & Bhurchandi, K. M., "Expression invariant face recognition using local binary patterns and contourlet transform", *Optik*, Vol. 127, No. 5, 2670-2678, 2016.

[36] Biswas, S., & Sil, J., "An efficient face recognition method using contourlet and curvelet transform". J*ournal of King Saud University-Computer and Information Sciences.* Vol. 32, No. 6, pp.718-729. 2020.

[37] Chitaliya, N. G., & Trivedi, A. I., "An efficient method for face feature extraction and recognition based on contourlet transforms and principal component analysis", *Procedia Computer Science*, Vol. 2, pp. 52-61, 2010.

[38] Abdolali, F., Zoroofi, R. A., Otake, Y., & Sato, Y., "Automated classification of maxillofacial cysts in cone beam CT images using contourlet transformation and Spherical Harmonics". *Computer methods and programs in biomedicine,* Vol.139, pp. 197-207, 2017.

[39] Alaei, F., Alaei, A., Pal, U., & Blumenstein, M., "A comparative study of different texture features for document image retrieval". *Expert Systems with Applications*, Vol. 121, pp. 97-114, 2019.

[40] Acharya, U. R., Raghavendra, U., Koh, J. E., et.al., "Automated detection and classification of liver fibrosis stages using contourlet transform and nonlinear features", *Computer Methods and Programs in Biomedicine*, Vol. 166, pp. 91-98, 2018.

[41] Chen, G. Y., & Kégl, B., "Invariant pattern recognition using contourlets and AdaBoost", *Pattern Recognition*, Vol. 43, No. 3, pp. 579-583, 2010.

[42] Das, D. K., Koley, S., Bose, S., Maiti, A. K., Mitra, et.al., "Computer aided tool for automatic detection and delineation of nucleus from oral histopathology images for OSCC screening", *Applied Soft Computing*, Vol. 83, 2019.

[43] Zhang, Q., Song, S., Xiao, Y., Chen, S., Shi, J., & Zheng, H., "Dual-mode artificially intelligent diagnosis of breast tumours in shear-wave elastography and B-mode ultrasound using deep polynomial networks", *Medical Engineering & Physics*, Vol. 64, pp. 1-6, 2019.

[44] Selvapandian, A., & Manivannan, K., "Fusion based glioma brain tumor detection and segmentation using ANFIS classification". *Computer Methods and Programs in Biomedicine*, Vol. 166, pp. 33-38, 2018.

[45] Amorim, P., Moraes, T., Fazanaro, D., Silva, J., & Pedrini, H., "Shearlet and contourlet transforms for analysis of electrocardiogram signals", *Computer Methods and Programs in Biomedicine*, Vol. 161, pp. 125-132, 2018.

[46] Wang, J., Li, Q., Jia, Z., Kasabov, N., & Yang, J., "A novel multi-focus image fusion method using PCNN in nonsubsampled contourlet transform domain". *Optik*, Vol. 126, No. 20, pp. 2508-2511, 2015.

[47] Yin, H., Liu, Z., Fang, B., & Li, Y., "A novel image fusion approach based on compressive sensing", *Optics Communications*, Vol. 354, pp. 299-313, 2015.

[48] Anandhi, D., & Valli, S., "An algorithm for multi-sensor image fusion using maximum posteriori and nonsubsampled contourlet transform", *Computers & Electrical Engineering*, Vol. 65, pp. 139-152, 2018.

[49] Chai, Y., Li, H., & Zhang, X., "Multifocus image fusion based on features contrast of multiscale products in nonsubsampled contourlet transform domain". *Optik*, Vol. 123, No. 7, pp. 569-581, 2012.

[50] Chen, Y., Xiong, J., Liu, H. L., & Fan, Q. "Fusion method of infrared and visible images based on neighborhood characteristic and regionalization in NSCT domain", *Optik*, Vol. 125, No 17, pp. 4980-4984, 2014.

[51] Chen, Y., & Sang, N., "Attention-based hierarchical fusion of visible and infrared images", *Optik*, Vol. 126, No. 23, pp. 4243-4248, 2015.

[52] Liu, C., Long, Y., & Mao, J., "Energy-efficient multi-focus image fusion based on neighbor distance and morphology". *Optik*, Vol.127, No. 23, pp. 11354-11363, 2016.

[53] Wang, K., "Rock particle image fusion based on sparse representation and non-subsampled contourlet transform". *Optik*, Vol. 178, pp. 513-523, 2019.

[54] Prakash, O., Park, C. M., Khare, A., Jeon, M., & Gwak, J., "Multiscale fusion of multimodal medical images using lifting scheme based biorthogonal wavelet transform", *Optik*, Vol. 182, pp. 995-1014, 2019.

[55] Gho, S. M., Nam, Y., Zho, S. Y., Kim, E. Y., & Kim, D. H., "Three-dimension double inversion recovery gray matter imaging using compressed sensing", *Magnetic Resonance Imaging*, Vol. 28, No. 10, pp. 1395-1402, 2010.

[56] Yang, X., Xu, W., Luo, R., Zheng, X., & Liu, K. "Robustly reconstructing magnetic resonance images via structure decomposition". *Magnetic Resonance Imaging*, Vol. 57, pp. 165-175, 2019.

[57] Yin, M., Liu, W., Zhao, X., Guo, Q. W., & Bai, R. F. "Image denoising using trivariate prior model in nonsubsampled dual-tree complex contourlet transform domain and non-local means filter in spatial domain", *Optik*, Vol. 124, No. 24, pp. 6896-6904, 2013.

[58] Li, D. M., Zhang, L. J., Yang, J. H., & Su, W. "Research on wavelet-based contourlet transform algorithm for adaptive optics image denoising". *Optik*, Vol. 127 No. 12, pp. 5029-5034, 2016.

[59] Guo, D., & Chen, J., "The application of contourlet transform to image denoising", *Procedia Engineering*, Vol. 15, pp. 2333-2338, 2011.

[60] Wang, X., Song, R., Mu, Z., & Song, C., "An image NSCT-HMT model based on copula entropy multivariate Gaussian scale mixtures", *Knowledge-Based Systems*, Vol. 193, 2020.

[61] Lyu, Z., Zhang, C., & Han, M., "A nonsubsampled countourlet transform based CNN for real image denoising". *Signal Processing: Image Communication*, Vol. 82, 2020.

[62] Eslami, R., & Radha, H., "The contourlet transform for image denoising using cycle spinning". *In 37th Asilomar Conference on Signals, Systems & Computers*, Vol. 2, pp. 1982-1986, 2003.

[63] Wang, X. Y., Yang, H. Y., Zhang, Y., & Fu, Z. K. "Image denoising using SVM classification in nonsubsampled contourlet transform domain", *Information Sciences*, Vol. 246, pp. 155-176, 2013.

[64] Sivakumar, R., Balaji, G., Ravikiran, R. S. J., Karikalan, R., & Janaki, S. S., "Image denoising using contourlet transform", *In 2009 Second International Conference on Computer and Electrical Engineering*, Vol. 1, pp. 22-25, 2009.

[65] Krishnamoorthi, R. (2012). "A multiresolution approach for rotation invariant texture image retrieval with orthogonal polynomials model". *Journal of Visual Communication and Image Representation*, Vol. 23, No. 1, 18-30, 2012.

[66] Li, L., Yuan, X., Lu, Z., & Pan, J. S. (2010). "Rotation invariant watermark embedding based on scale-adapted characteristic regions". *Information Sciences*, Vol. 180, No. 15, pp. 2875-2888, 2010.

[67] Wang, X. Y., Zhang, S. Y., Wen, T. T., Yang, H. Y., & Niu, P. P., "Coefficient difference based watermark detector in nonsubsampled contourlet transform domain". *Information Sciences*, Vol. 503, pp. 274-290, 2019.

[68] Etemad, S., & Amirmazlaghani, M., "A new multiplicative watermark detector in the contourlet domain using t Location-Scale distribution". *Pattern Recognition*, Vol. 77, pp. 99-112, 2018.

[69] Kumar, S. S., Moni, R. S., & Rajeesh, J. "An automatic computer-aided diagnosis system for liver tumours on computed tomography images", *Computers & Electrical Engineering*, Vol. 39, No. 5, pp. 1516-1526, 2013.

[70] Yapi, D., Mejri, M., Allili, M. S., & Baaziz, N., "A learning-based approach for automatic defect detection in textile images". *IFAC-PapersOnLine,* Vol. 48, No. 3, pp. 2423-2428, 2015.

[71] J.G. Daugman, "Uncertainty relations for resolution in space, spatial frequency, and orientation optimized by two-dimensional visual cortical filters", *Journal of the Optical Society of America*, Vol. 2, pp. 1160-1169, 1985.

[72] Wang, X., Ding, X., & Liu, C., "Gabor filters-based feature extraction for character recognition", *Pattern Recognition*, Vol. 38, No. 3, 369-379, 2005.

[73] Samantaray, A. K., & Rahulkar, A. D., "New design of adaptive Gabor wavelet filter bank for medical image retrieval". *IET Image Processing*, Vol. 14, No. 4, pp. 679-687, 2019.

[74] Yuan, Y., Zhang, J. A., & Wang, Q., "Deep Gabor convolution network for person re-identification", *Neurocomputing*, Vol. 378, pp. 387-398, 2020.

[75] Fathi, A., Alirezazadeh, P., & Abdali-Mohammadi, F., "A new Global-Gabor-Zernike feature descriptor and its application to face recognition", *Journal of Visual Communication and Image Representation*, Vol. 38, pp. 65-72, 2016.

[76] Dora, L., Agrawal, S., Panda, R., & Abraham, A., "An evolutionary single Gabor kernel-based filter approach to face recognition". *Engineering Applications of Artificial Intelligence*, Vol.62, pp. 286-301, 2017.

[77] Muthukumar, A., & Kavipriya, A., "A biometric system based on Gabor feature extraction with SVM classifier for Finger-Knuckle-Print". *Pattern Recognition Letters*, Vol. 125, pp. 150-156, 2019.

[78] Pichler, O., Teuner, A., & Hosticka, B. J., "A comparison of texture feature extraction using adaptive Gabor filtering, pyramidal and tree structured wavelet transforms". *Pattern Recognition*, Vol. 29, No. 5, pp. 733-742, 1996.

[79] Kong, W. K., Zhang, D., & Li, W., "Palmprint feature extraction using 2-D Gabor filters". *Pattern Recognition*, Vol. 36, No. 10, 2339-2347, 2003.

[80] Abhishree, T. M., Latha, J., Manikantan, K., & Ramachandran, S., "Face recognition using Gabor filter based feature extraction with anisotropic diffusion as a pre-processing technique". *Procedia Computer Science*, Vol. 45, pp. 312-321, 2015.

[81] Kim, N. C., & So, H. J., "Directional statistical Gabor features for texture classification". *Pattern Recognition Letters*, Vol. 112, pp. 18-26, 2018.

[82] Xing, Y., & Luo, W., "Facial expression recognition using local Gabor features and adaboost classifiers", In International Conference on Progress in Informatics and Computing, pp. 228-232, 2016.

[83] Islam, B., Mahmud, F., Hossain, A., Mia, M. S., & Goala, P. B., "Human Facial Expression Recognition System Using Artificial Neural Network Classification of Gabor Feature Based Facial Expression Information", *In 4th International Conference on Electrical Engineering and Information & Communication Technology*, pp. 364-368, 2018.

[84] Dewi, R. R. K., Sthevanie, F., & Arifianto, A. (2019, March). "Face expression recognition using Local Gabor Binary Pattern Three Orthogonal Planes (LGBP-TOP) and Support Vector Machine (SVM) method", *In Journal of Physics: Conference Series*, Vol. 1192, No. 1, pp. 12-48, 2019.

[85] NAUSHAD1290, "Image Processing and Computer vision in java (Image Filtering part1)", [Online]. Available: https://naushadsblog.wordpress.com/2014/04/25/image-processing-and-computer-vision-in-java-image-filtering-part1/. [Accessed 06.06.2021]

[86] A. Domínguez, "Highlights in the History of the Fourier Transform [Retrospectroscope]", *IEEE Pulse*, Vol. 7, No. 1, pp. 53-61, 2016.

[87] Li, J., Levine, M. D., An, X., Xu, X., & He, H., "Visual saliency based on scale-space analysis in the frequency domain". *IEEE Transactions on Pattern Analysis and Machine Intelligence*, Vol. 35, No. 4, pp. 996-1010, 2012.

[88] Jain, P., & Tyagi, V., "Spatial and frequency domain filters for restoration of noisy images", *IETE Journal of Education*, Vol. 54, No. 2, pp. 108-116, 2013.

[89] Choi, S. E., Lee, Y. J., Lee, S. J., Park, K. R., & Kim, J., "A comparative study of local feature extraction for age estimation", *11th International Conference on Control Automation Robotics & Vision*, pp. 1280-1284, 2010.

[90] Freeman, W. T., & Adelson, E. H., "The design and use of steerable filters", *IEEE Transactions on Pattern Analysis and Machine Intelligence*, Vol. 13, No. 9, 891-906, 1991.

[91] Burt PJ, Adelson EH. "The Laplacian Pyramid as a compact image code", *IEEE Transactions on Communications*, Vol. 31, No. 4, pp. 532-40, 1983.

[92] Da Cunha, A. L., Zhou, J., & Do, M. N. (2006). "The nonsubsampled contourlet transform: theory, design, and applications", *IEEE Transactions on Image Processing*, Vol. 15, No. 10, pp. 3089-3101, 2006.

[93] P. Ekman, W.V. Friesen, "Facial action coding system (FACS): A technique for the measurement of facial actions", *Rivista Di Psichiatria* Vol. 47, No.2, pp. 126–138, 1978.

[94] Xie, W., Jia, X., Shen, L., & Yang, M., "Sparse deep feature learning for facial expression recognition", *Pattern Recognition*, Vol.96, 2019.

[95] Shao, J., & Qian, Y., "Three convolutional neural network models for facial expression recognition in the wild", *Neurocomputing*, Vol. 355, pp. 82-92, 2019.

[96] Barman, A., & Dutta, P. (2017). "Facial expression recognition using distance and shape signature features", *Pattern Recognition Letters*. Vol. 145, pp.254-261, 2021.

[97] Hernandez-Matamoros, A., Bonarini, A., Escamilla-Hernandez, E., Nakano-Miyatake, M., & Perez-Meana, H., "Facial expression recognition with automatic segmentation of face regions using a fuzzy based classification approach". *Knowledge-Based Systems*, Vol. 110, pp. 1-14, 2016.

[98] Biswas, S., & Sil, J., "An efficient expression recognition method using contourlet transform", *In Proceedings of the 2nd International Conference on Perception and Machine Intelligence*, pp. 167-174, 2015.

[99] Jabid, T., Kabir, M. H., & Chae, O. "Robust facial expression recognition based on local directional pattern". *ETRI Journal*, Vol. 32, No. 5, pp. 784-794, 2010.

[100] A. Navlani, "Support Vector Machines with Scikit-learn", [Online]. Available: https://www.datacamp.com/community/tutorials/svm-classification-scikit-learn-python. [Accessed 01 07 2021].

[101] V. Lyashenko "Cross-Validation in Machine Learning: How to Do It Right", [Online]. Available: "https://neptune.ai/blog/cross-validation-in-machine-learning-how-to-do-it-right. [Accessed 01 07 2021].

[102] Dagher, I., Dahdah, E., & Al Shakik, M., "Facial expression recognition using three-stage support vector machines",*Visual Computing for Industry, Biomedicine, and Art*, Vol. 2, No. 1, pp. 1-9, 2019.

[103] Sun, Y., & Yu, J., "Facial expression recognition by fusing Gabor and local binary pattern features". *In International Conference on Multimedia Modeling* pp. 209-220, 2017.